

Confined Flow: Consequences and Implications for Bacteria and Biofilms

Jacinta C. Conrad and Ryan Poling-Skutvik

Department of Chemical and Biomolecular Engineering, University of Houston, Houston, Texas 77204, USA; email: jcconrad@uh.edu

Annu. Rev. Chem. Biomol. Eng. 2018. 9:175–200

First published as a Review in Advance on
March 21, 2018

The *Annual Review of Chemical and Biomolecular
Engineering* is online at chembioeng.annualreviews.org

<https://doi.org/10.1146/annurev-chembioeng-060817-084006>

Copyright © 2018 by Annual Reviews.
All rights reserved

Keywords

swimming, twitching, surface attachment, biofilm mechanics, quorum sensing, mass transport

Abstract

Bacteria overwhelmingly live in geometrically confined habitats that feature small pores or cavities, narrow channels, or nearby interfaces. Fluid flows through these confined habitats are ubiquitous in both natural and artificial environments colonized by bacteria. Moreover, these flows occur on time and length scales comparable to those associated with motility of bacteria and with the formation and growth of biofilms, which are surface-associated communities that house the vast majority of bacteria to protect them from host and environmental stresses. This review describes the emerging understanding of how flow near surfaces and within channels and pores alters physical processes that control how bacteria disperse, attach to surfaces, and form biofilms. This understanding will inform the development and deployment of technologies for drug delivery, water treatment, and antifouling coatings and guide the structuring of bacterial consortia for production of chemicals and pharmaceuticals.



ANNUAL REVIEWS Further

Click here to view this article's
online features:

- Download figures as PPT slides
- Navigate linked references
- Download citations
- Explore related articles
- Search keywords

1. INTRODUCTION

Biofilm:

3D surface-associated communities of bacteria surrounded by a protective matrix of biopolymers

Planktonic:

floating or swimming as individual cells in liquid

Bacteria inhabit nearly every niche on earth, from the hydrothermal vents in the ocean depths to the frosty soils of the arctic tundra. Across the multitude of environments inhabited by bacteria, interactions with nearby surfaces play an essential role in determining bacterial behavior. Indirect interactions with surfaces are mediated by the fluids that deliver nutrients and through which bacteria move and are transported. Through direct interactions, bacteria use filamentous appendages to transiently move along surfaces and permanently attach there to form biofilms.

Fundamental for their ecology in native habitats, the behavior of bacteria under flow near surfaces or in confinement also informs the design and control of industrial processes. Bacteria such as *Escherichia coli* are crucial to the production of pharmaceuticals and proteins using recombinant DNA technology, especially for insulin (1) and modern cancer-targeting drugs (2). Microbial production requires flow near surfaces—traditional batch bioreactors are stirred or bubbled to distribute nutrients evenly, and modern perfusion bioreactors are continuously flushed with nutrients to improve production efficiency. Designing new processes to produce pharmaceuticals using bacteria relies on high-throughput screening methods to rapidly iterate through many parameters. As examples, flow cytometry (3) and microbioreactors (4) require controlling the flow, transport, sequestration, and identification of individual bacteria, often using microfluidic technology. How confinement and flow in these settings affect bacterial growth and transport remains incompletely understood.

Whereas bacterial growth is essential for pharmaceutical production, undesired bacterial growth is detrimental for other industries and processes. Bacteria readily colonize nearly any engineered or natural surface, using their surface appendages to attach and spread on surfaces of varying chemistry and topography (5). Attached bacteria subsequently divide and excrete polymeric substances to form a biofilm, a major contributor to the costly fouling of biomedical devices, bioreactors, food and paper processing equipment, membranes, and pipelines. Biofilms are estimated to generate annual costs of \$1–\$2 billion/year in corrosion damage and \$94 billion/year in healthcare. The high specific surface areas of confined materials exacerbate attachment and biofilm growth.

The affinity of bacteria for surfaces, so often targeted by antifouling materials, can be harnessed in creative and useful ways. Bacteria can act as microscale motors by adhering to and propelling payloads with modified surface chemistries (6). Microfabricated chemical (7) or topographic (8) patterns can generate ordered arrangements of adhered bacteria with well-defined spatial structure, with important implications for engineering functional synthetic consortia (9). Both shear forces from flow and adhesive forces to the surface modulate patterns of adhesion and motility of bacteria.

Beyond engineering applications, the motion and transport of bacteria through confined spaces affect diverse environmental and physiological processes. For example, bacterial pathogens may thrive in narrow pore throats and small voids between particles of soil (10) or permeate tight gaps between cells to invade tissues (11). Although invasion of pathogenic bacteria can lead to diseases such as tuberculosis and pneumonia, bacteria can also serve as drug delivery vectors (12) due to their ability to swim and move collectively through narrow vasculature and crowded tissue. Despite the relevance for a wide array of engineering problems, fundamental questions remain about the role of fluid flow and confinement on behavior of planktonic and surface-attached bacteria.

This review focuses on bacterial behaviors arising from the interplay of geometric confinement and flow. This focus complements recent reviews that more broadly describe effects of flow for planktonic bacteria (13–15) and biofilms (16, 17) or that describe new approaches to generate confined microenvironments (18). By broadly considering the consequences of confined flow over a range of bacterial densities, we highlight the relevance of confined flow across the biofilm developmental process.

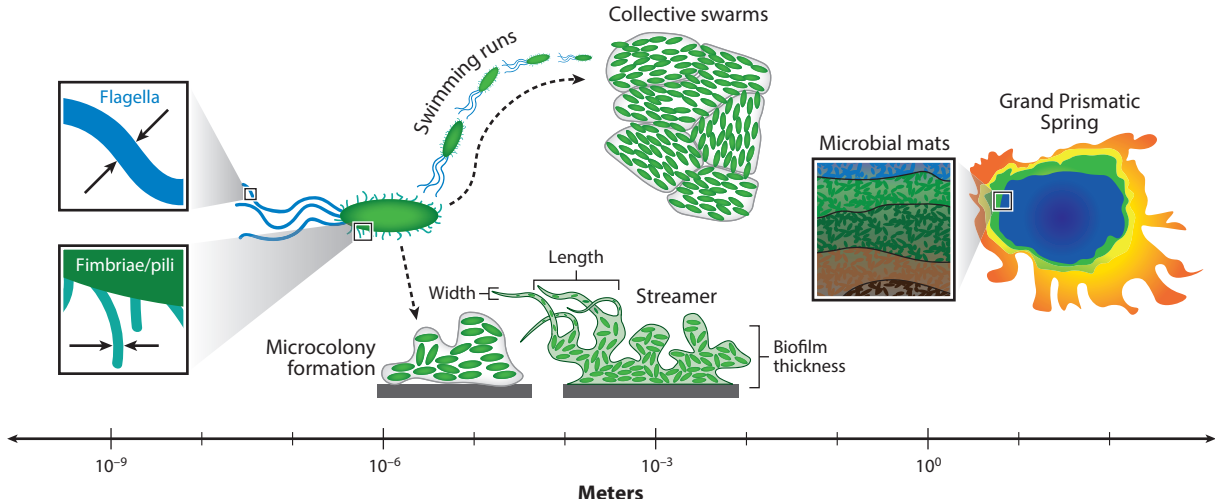


Figure 1

Relevant length scales for bacteria. Filamentous appendages (i.e., flagella and pili, of width 1–10 nm and length 1–10 μ m) on the surface of bacteria (length and width usually between 0.3–3 μ m) facilitate movement of bacteria (straight run lengths are up to 30 μ m in length) and their arrangement into complex structures near surfaces (e.g., microcolonies, 10–1,000 μ m in size, and biofilms, of thickness 10–1,000 μ m) or in fluids (e.g., collective swarms, of size 10–1,000 μ m). Biofilms and microbial mats, e.g., in the Grand Prismatic Spring in Yellowstone National Park, USA, can exceed 1–10 m in size.

2. CONFINED FLOW

2.1. Length Scales for Bacteria

Bacteria possess or collectively organize into structures ranging from nanometers to many meters in size (Figure 1). The length scales of their surface filamentous appendages, for example, are comparable to the dimensions of dialysis (2–5 nm) and ultrafiltration (2–100 nm) membranes. The body size of bacteria is comparable to characteristic pore sizes within soils (1–10 μ m, for loams) or to the wide array of pore sizes in the extracellular matrix (1–10 μ m). The directional persistence of individual swimming bacteria and the size scales characterizing the collective motility of swimming, swarming, or twitching bacteria are comparable to the inner diameters of catheters (90 μ m and greater), as are the characteristic sizes of microcolonies. Biofilm thicknesses are comparable to the diameter of medical and industrial tubing (\geq 1 mm), although their lateral dimensions can be much larger—indeed, environmental biofilms can span many meters. This broad range of relevant length scales, spanning orders of magnitude, illustrates the challenge in describing effects arising from the interaction of confinement and flow.

From a materials perspective, geometric confinement becomes relevant when the confining dimension b of a material is within an order of magnitude of a characteristic length scale L —here, of appendages, cells, runs, swarms, colonies, or biofilms. The ratio between bacterial and material length scales can serve as an effective confinement parameter $\zeta = L/b$, with changes in bacterial behavior expected from this argument when ζ becomes of order ten or lower. Although not confined by a strict definition, nearby surfaces may modulate the dynamics of bacteria through chemical, steric, and/or hydrodynamic interactions—each with a characteristic interaction range. Chemical and steric interactions are typically short-ranged, acting over nanometers, whereas hydrodynamic interactions depend sensitively on the details of the flow field within the fluid. For

Twitching: collective motility mode in which bacteria move together in a jerky fashion to rapidly spread on a surface

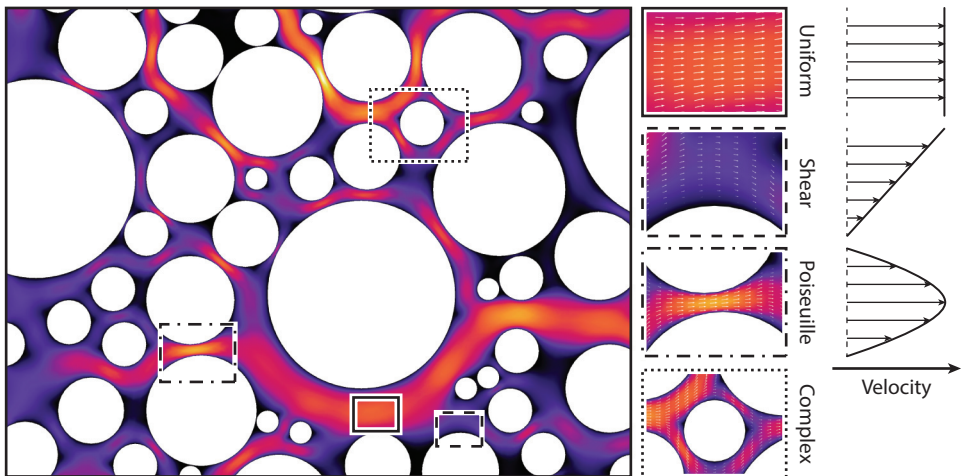


Figure 2

Schematic of simulated fluid flow through random porous media. Expanded boxes highlight the variety of velocity profiles that can develop: uniform (*solid*), shear (*dashed*), and Poiseuille (*dot-dashed*). Corresponding velocity profiles are sketched to the right. These regimes occur in the absence of confinement, 0D confinement near a wall, and 1D confinement between walls, respectively. More complex profiles (*dotted*) develop in complex geometries.

one simple case, diffusion of a microscale sphere near a surface, hydrodynamic interactions decay inversely with the distance from the surface (e.g., $\sim R^{-1}$). These comparisons suggest that physicochemical surface interactions act over length scales shorter than or comparable to appendages and cells.

2.2. A Prototypical Example of Confined Flow

Solid interfaces alter fluid flow profiles by introducing classical no-slip boundary conditions, at which the velocity of the fluid approaches zero. The shape of the velocity profile within the fluid depends on the arrangement of these interfaces. Treating a tortuous porous medium as a bulk continuum with an effective porosity and permeability, Darcy's and Brinkman's laws describe the average flux through the medium. On local length scales, however, the heterogeneous structure of porous media can cause any of a variety of potential velocity profiles to develop (Figure 2). Far from any interfaces the fluid may flow as a plug, with a spatially uniform velocity profile. Near a single surface, the velocity profile is nearly linear, increasing away from the interface. When constricted between interfaces, such as a pore throat, the fluid adopts a parabolic velocity profile similar to that in fully developed Poiseuille flow. In more complex geometries within the media, fluid flow is multidirectional without a simple mathematical description. Constrictions through pore throats and dilations into interstitial spaces introduce an extensional component to the flow.

Beyond structural heterogeneities, fluid rheology drastically affects the flow field through confined porous media. Liquids encountered in microbiology often exhibit non-Newtonian features. One example of a non-Newtonian fluid is a solution of polymers, such as the polysaccharides found in the extracellular matrix of biofilms. The viscosity of many polymer solutions decreases as the shear rate is increased over an intermediate range, as polymer chains elongate and align in flow. This shear-dependent viscosity leads to deviations in the velocity profiles of polymer solutions from the classical profiles derived for Newtonian fluids, especially near interfaces.

2.3. Confined Flow and Transport of Colloids

To understand how bacteria move with flow through confined geometries, we first consider the transport of colloids and nanoparticles, whose dynamics should be similar to those of nonmotile bacteria (such as the skin bacterium *Staphylococcus epidermidis*). When flowed in a straight and rigid channel, colloidal particles with hard-sphere or repulsive interactions undergo biased diffusion, driving them to migrate toward the region of lowest shear rate at the channel center (19). This shear-induced migration is most pronounced at high volume fractions of colloids and when advection is strong compared to particle diffusion, quantitatively described by a large Péclet number (the ratio of the advection and diffusion rates). Theoretical models posit that gradients in the stress tensor drive particle migration (20). Addition of polymers to the suspension may reduce particle migration, by promoting aggregation through entropic depletion interactions that maximize the free volume available to the polymers (21), or enhance it, through demixing of particles and polymers (22), depending on the particle and polymer concentrations and the flow rate.

The finite size of colloids and nanoparticles constrains their motion within confined porous media, leading to unexpected transport properties. In a geometrically ordered medium, for example, particles of carefully tuned sizes can be regularly displaced from streamlines to generate deterministic particle trajectories (23). In other settings, geometric order couples advective and diffusive particle transport on short time- and length scales (24). Both mechanisms alter how particles disperse through the medium. Furthermore, particles may be excluded by their size from accessing the slowest streamlines near the surface of obstacles or channels (25), manifesting at the macroscopic (column) scale as early breakthrough (26). These phenomena affecting colloidal transport in confinement derive largely from hard-sphere repulsions between the colloids and the confining surfaces, but softer repulsive potentials will also affect microparticle transport.

Soft confinement occurs when micro- and nanoparticles are dispersed in complex fluids containing polymers, proteins, or other macromolecules, which are collectively termed crowders because they reduce the free volume available to the particles. These crowders are usually mobile, create finite attractive potentials of order $1-10 k_B T$ between particles, and introduce structural heterogeneities over the micron and submicron length scales that affect diffusive and advective transport. In a purely viscous solvent, colloids and nanoparticles undergo Brownian diffusion with a diffusivity described by the Stokes-Einstein equation. Heterogeneities present in crowded fluids may generate deviations from the Stokes-Einstein diffusivity. When particles are much larger than characteristic length scales in the crowder solution (for example, the size or separation between crowders), particle dynamics couples to viscoelastic relaxations of the complex fluid (27). When particles are comparable in size to these crowder length scales, however, anomalous diffusion is often observed. In this regime, particle dynamics may couple to relaxation modes of the crowders themselves (28, 29), reflect transient caging by mobile crowders (30), and/or reflect transient immobilization driven by macromolecule-mediated interactions with surfaces (31). Because the size of bacteria and their appendages also falls in this regime, their motility is expected to be affected by crowders and their relaxations. Second-order effects arise when particle-laden complex fluids are flowed through confined media. In ordered geometries, polymer additives enhance hydrodynamic dispersion of particles (relative to Newtonian fluids) because the periodic order regularly augments transverse displacements generated by shear-induced deformation of the polymers (32, 33). Disordered geometries, however, average out polymer-induced fluctuations and do not lead to significant differences in particle dispersion (34).

3. SWIMMING

Unlike passive colloids and nanoparticles, many bacteria actively move by swimming using one or more flagella (35). Swimming is especially widespread for pathogenic bacteria, allowing the food pathogen *Salmonella enterica* to approach host surfaces prior to infection (36) and enhancing the virulence of the enteric pathogen *E. coli* as it invades the urinary tract (37). These infectious processes necessarily involve interactions of swimming bacteria with nearby surfaces. Methods to fabricate microfluidic devices on length scales of 10–1,000 μm have expanded opportunities for probing microbiology near surfaces or confined in one (plates) or two (channels, **Figure 2**) dimensions (38). Here, we describe how nearby surfaces modify bacterial swimming, emphasizing the effects of flow (**Figure 3**).

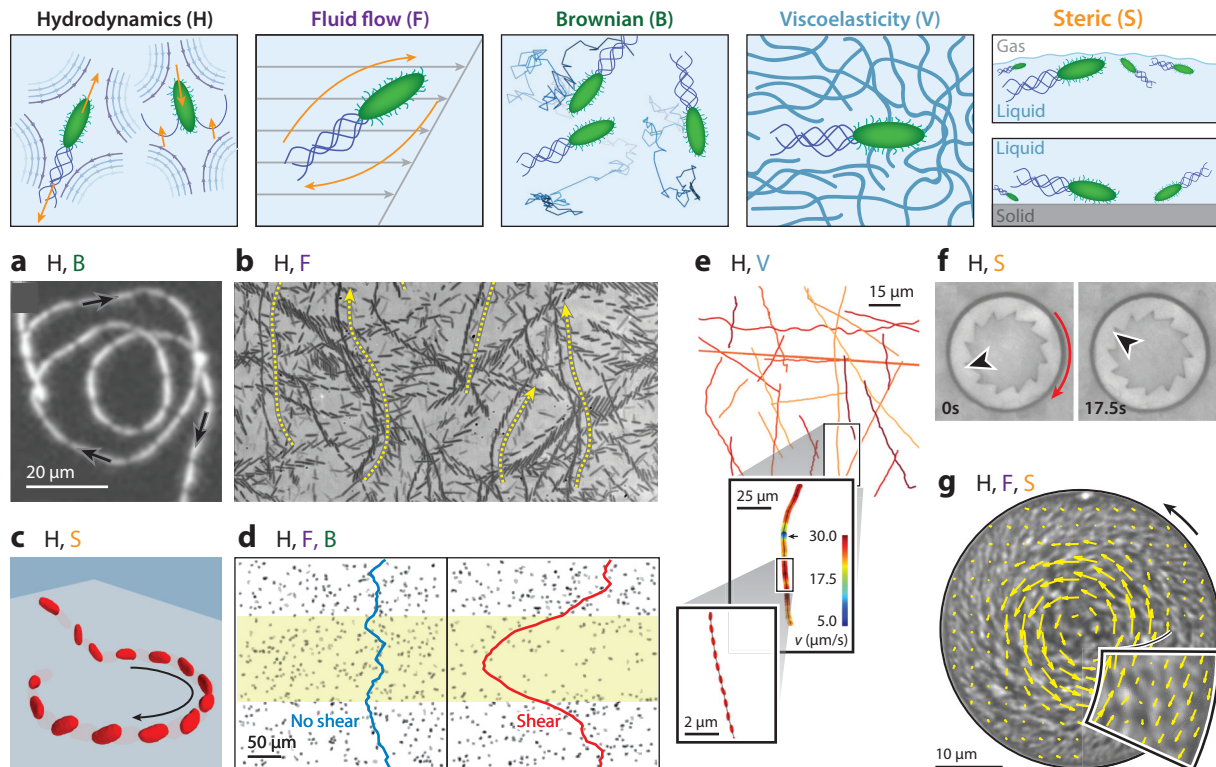


Figure 3

Multiple types of interactions modify the swimming behavior of bacteria. (Top row) These include hydrodynamic interactions (H) arising from the active motion of bacteria, external fluid flow (F), Brownian motion (B), fluid viscoelasticity (V) due to crowders or other macromolecules, and steric interactions (S) with nearby surfaces. (a) Circular trajectory of *Caulobacter crescentus* swimming near a solid surface (reproduced with permission from Reference 52, copyright 2008 National Academy of Sciences, USA). (b) Upstream swimming in *Escherichia coli* (reproduced with permission from Reference 58, copyright 2012 Biophysical Society). (c) Surface approach and wall entrapment of *E. coli* (reproduced from Reference 53 and available under the terms of the Creative Commons Attribution 3.0 License). (d) Shear-induced depletion of *Bacillus subtilis* near the center of a microchannel, with curves indicating the concentration of bacteria in the absence of (blue) and under (red) shear flow (reproduced with permission from Reference 66, copyright 2014 Macmillan Publishers Ltd.). (e) Linear trajectories of *E. coli* bacteria swimming in polymer solutions (reproduced from Reference 86 and available under the terms of the Creative Commons Attribution 4.0 License). (f) Rotational motion of a microscale gear driven by collective swimming of *B. subtilis* (reproduced with permission from Reference 69). (g) Steady-state circulation of *B. subtilis* confined within a water droplet with arrows indicating relative velocities (reproduced from Reference 73 and available under the terms of the Creative Commons Attribution 3.0 License).

Bacteria are low-Reynolds number swimmers [from characteristic length scales and swimming velocities in **Figure 1**, the ratio of inertial and viscous forces is $Re \sim 10^{-5}$ (35)], with motion dominated by the viscosity of the fluid in which they swim. In this limit, the Stokes equations require propulsion mechanisms to be nonreversible in time. The great majority of bacteria swim using one or more flagella, consisting of a passive helical filament connected to a rotary motor. For example, *E. coli* bears many flagella, distributed about its body, that assemble into a bundle for swimming. *Caulobacter crescentus*, a model organism for cell cycle regulation, and *Pseudomonas aeruginosa*, an opportunistic pathogen and model organism for biofilm formation, each bear one polar flagellum; *Rhodobacter sphaeroides*, a model organism for photosynthesis, bears one lateral flagellum. Hydrodynamic drag on the filament, driven by motor rotation at ~ 100 Hz, generates a net viscous force along the axis of the helix that propels the cell forward; counterrotation of the cell body at ~ 25 Hz leads to the force- and torque-free swimming required at low Re in the absence of external forces (39).

Flagellum:
helical filament whose
rotational motion
allows bacteria to swim

3.1. Near-Surface Swimming and Accumulation

Far from surfaces, flagellated bacteria swim in approximately straight lines and change direction using one of several mechanisms, depending on the number and location of their flagella. *E. coli* reverses the direction of motor rotation, unbundling the flagella and generating a tumble. *C. crescentus* also reverses the direction of motor rotation for its single flagellum, whereas *R. sphaeroides* halts motor rotation entirely. Near no-slip solid surfaces, however, flagellated bacteria swim in clockwise circles (40). These curved trajectories result from hydrodynamic forces and moments induced by surfaces (41). Both the rotating helix and the counterrotating cell body experience hydrodynamic forces that decrease with distance from the surface, leading to a wall-induced moment that rotates the bacterium (42). Hydrodynamic models predict the curvature of the trajectory to decrease and the swimming speed to increase as bacteria swim farther from the surface (41). The direction of the surface-induced moment depends on the boundary conditions at the interface. Near air-water interfaces for which slip boundary conditions hold, bacteria swim in counterclockwise circles (43). Thus, the change in the curvature direction can be exploited to direct microbial motility near patterned surfaces (44) or to probe interfacial properties (45).

As a second example of how nearby surfaces modify swimming behaviors, bacteria such as *E. coli* (46) and *C. crescentus* (47) accumulate near surfaces. This increase in density near surfaces is driven, in part, by an increase in the near-surface residence time (48). The increase in residence time was first attributed to the hydrodynamic interactions of a flagellated swimmer with the surface (49). A flagellated bacterium generates a positive dipolar flow in the surrounding fluid, repelling fluid along its long axis and pulling fluid in along its side. At distances greater than a few cell body lengths, however, this bacteria-driven flow is overwhelmed by thermal noise (50). This result indicates that short-range steric interactions, arising when bacteria collide with surfaces, strongly influence accumulation. Collisions with the surface reorient bacteria and align them parallel to the surface (51), leading to an increase in bacterial density there; Brownian fluctuations reorient bacteria and reduce accumulation (50, 52) (**Figure 3a**). Although steric collisions initiate reorientation at the surface, the nose-down orientation of cells swimming along a surface suggests that near-field hydrodynamic coupling is essential for maintaining a near-wall trajectory (53) (**Figure 3c**). Similarly, near-field hydrodynamic contributions that reorient bacteria into the surface (54) likely contribute to trapping of *E. coli* near convex obstacles (55).

Flows near surfaces in environmental and physiological settings generate shear rates of order 1–10/s in soils and 10–1,000/s within the body. Under fluid shear conditions, bacterial locomotion does not have to be force and torque free. Indeed, linear fluid shear can generate torques on bacteria

Rheotaxis: changes in an organism's motility in response to fluid shear

or their appendages, modifying their direction of motion. As one example, near-surface simple shear flows periodically reorient nonflagellated *E. coli* along their fore-aft axis (56). The trajectories of the bacteria are described by Jeffery's theory, which predicts the motion of prolate spheroids in a steady linear shear flow in the absence of inertia (57). The orbital period increases as bacteria move closer to the wall and experience greater hydrodynamic interactions (56). As a second example, flagellated bacteria such as *E. coli* (58) (**Figure 3b**) and *Bacillus subtilis* (59) can exhibit rheotaxis and swim upstream against shear flow. Far from surfaces, shear-induced torques on the helical filament can reorient bacteria to drift across streamlines (59). Near surfaces, shear flow at moderate rates [$\sim 100/\text{s}$ (58)] can reorient the body of the bacterium to swim against the flow direction (60). *E. coli* confined (in 2D) in a channel swim upstream near the channel walls, where hydrodynamic interactions are greater (61). Simulations of a model run-and-tumble swimmer reveal that channel width and swimmer density sensitively affect swimmer velocity profiles (62). The ability to swim upstream arises from the interaction of flow-induced torques and bacterial motion and is not observed in passive anisotropic or helical colloids (which are still reoriented by flow).

The combination of bacterial motility and fluid shear affects the ability of bacteria to remain trapped near surfaces. Under quiescent conditions, hydrodynamic surface interactions reduce the frequency of the tumbles used by *E. coli* bacteria to change direction; bacteria that reorient remain aligned with the surface (63). Because the reduction in tumbling persists at distances from the surface of $20\ \mu\text{m}$, much greater than the length of a flagellum or bundle, hydrodynamic interactions between the flagella and the surface likely reduce the forces necessary to unbundle and thereby quench tumbles (63). Gentle shear flows (0.06–30/s), however, increase the tumbling frequency close to that measured in a bulk fluid, reflecting contributions of both passive reorientation and active shear-enhanced unbundling of flagella (64). Hence imposed flows can detach bacteria from the near-wall position (61). Competing effects from the external flow field and from the hydrodynamic interactions of a flagellated swimmer with the wall can either promote or hinder detachment; simulations suggest that the run-and-tumble motion of *E. coli* represents an effective strategy for surface escape, compared to enhancements in thermal noise that drive Brownian rotation (65). More generally, fluid shear alone can drive elongated bacteria to accumulate in regions of high shear often found near surfaces; by rotating bacteria to align along the flow direction, fluid shear suppresses their motility across a channel, independent of the mechanism used by a bacterium to change direction (66) (**Figure 3d**).

3.2. Collective Swimming

The interplay of fluid shear and bacteria-surface hydrodynamic and steric interactions that affects single cells near interfaces also affects collective swimming behaviors of bacteria. Near-wall accumulation, described in Section 3.1, provides one example of a collective behavior arising from fluid flow and surface interactions. In a second example, unconfined bacteria at high cell densities swim in self-organized patterns on length scales of $10\text{--}100\ \mu\text{m}$ (67). By markedly reducing the fluid viscosity, collective swimming can nearly eliminate viscous resistance to shear (68). Momentum transfer from collectively swimming bacteria to nearby surfaces, enhanced by the decrease in viscosity, can actuate macroscopic motions—rotating microscale gears (69) (**Figure 3f**) or propelling microscale arrows (70). Conversely, 1D confinement between planar walls may suppress this collective swimming (71).

Swimming bacteria themselves generate fluid flows that can drive accumulation in confined spaces. In thin colonies, *B. subtilis* bacteria move collectively in jets and whirls that are much larger ($10\text{--}100\ \mu\text{m}$) than individual cells and at speeds ($\sim 100\ \mu\text{m/s}$) that greatly exceed that of a single swimmer (72). In thin circular films, *B. subtilis* bacteria self-organize into a stable vortex, driven by

steric interactions within the boundary layer that orient the cells (73) (**Figure 3g**). Surprisingly, outward-pointing bacteria within the vortex swim upstream. The fluid pushed backward by their flagella generates the bulk flow in the film, and hydrodynamic interactions stabilize the vortex state (74). Similarly, bacteria confined in 2D in a thin oval racetrack channel undergo a transition from disordered to unidirectional swimming as the channel width is decreased below the correlation length measured in bulk fluid suspensions (75). The bacteria-driven fluid flow near the boundaries of the racetrack again drives this self-organization. Again, both steric and hydrodynamic interactions with confining geometries contribute to drive nonbulk swimming behaviors.

3.3. Porous Media

Bacteria in natural environments often interact with geometries that are more complex than thin films or channels, which feature 1D or 2D confinement. The schematic in **Figure 2** is an idealized representation of the pore space in soils or in the extracellular matrix, as two examples. Swimming may enhance (76) or reduce (77) the dispersion of bacteria flowed through porous media, depending on the strain of bacteria and the geometry of the medium. Motile bacteria can swim through throats that are only 30% larger than their size (78), and thus are able to access a large fraction of the void space within a porous medium. Nevertheless, geometrically complex confinements can modulate swimming behaviors. Multiply flagellated *B. subtilis*, for example, tumbles to change direction in bulk fluid but reverses direction upon encountering an obstacle (79). During reversal, it changes direction without reversing the orientation of its body, similar to the reversals observed in singly flagellated *Vibrio alginolyticus* (80). How interactions with obstacles affect the ability of bacteria to swim through a porous medium, though, is not fully understood. *E. coli* swimming in a quasi-2D disordered porous medium exhibit higher run-to-tumble frequencies that are consistent with more frequent changes in direction (81). Conversely, *Pseudomonas putida*, which lives in close-packed soils and bears multiple polar flagella, exhibits longer-than-expected runs when swimming through an ordered porous medium with throat sizes smaller than the bacterium and its flagella, despite frequent collisions (82). The contrast of these results suggests that geometric order may modulate the directional persistence of swimmers navigating a porous medium.

3.4. Complex Fluids

Bacteria in natural settings swim through complex fluids, such as natural organic matter (\sim 1–10 nm, flocs of up to 1 mm) and mucus (fibers of diameter \sim 100 nm, pore sizes of 100 nm–10 μ m), and excrete extracellular polymers. The heterogeneous structure of these fluids on that nano- to microscale is expected to alter bacterial motility (83). Moreover, characteristic timescales associated with bacterial motion (e.g., flagellar rotation, cell body translation) are comparable to those associated with relaxation processes in complex fluids. Thus, relaxations and dynamics of complex fluids may also alter bacterial motility.

Early experiments on bacterial motility in polymer solutions suggest that the swimming speed of *E. coli* decreases as polymer concentration is increased (84). Because the rotary motor operates at constant torque, the increase in (effectively, Newtonian) fluid viscosity obtained by adding small polymers is expected to decrease the swimming speed of *E. coli* (35). Larger polymers whose size exceeds that of the flagellar bundle (\sim 40 nm) relax on timescales comparable to the local shear generated by flagellar rotation; the local shear flow generated by the bundle falls within the shear-thinning regime of the polymer solution, leading to deviations from the Newtonian fluid prediction (85). Both viscous and elastic contributions to the flow can be accessed by tuning the concentration and molecular weight of the polymers in solution. Increasing the viscosity reduces

the frequency at which *E. coli* tumbles, whereas increasing the elasticity suppresses inefficient wobbling and thereby increases its swimming speed (86) (**Figure 3e**). Thus, nano-, micro-, and continuum-scale fluid properties can modulate the individual motility of bacteria in bulk fluids.

Because they affect hydrodynamic interactions of bacteria and appendages, complex fluids are also expected to modulate confined swimming behaviors. Simulations predict, for example, that fluid elasticity can increase the residence time of swimmers near surfaces (87) and can modify collective motion in bulk fluids (88). How flow of complex fluids affects the behavior of swimmers, however, has received surprisingly little attention—despite strong relevance for understanding the transport mechanisms of gastrointestinal pathogen *Helicobacter pylori* through the viscoelastic gut mucus (89) or the Lyme disease vector *Borrelia burgdorferi* through the extracellular fluid (90). For these processes, understanding how fluid rheology affects the accumulation of bacteria near confining surfaces has significant implications for the onset of infection. Recent theoretical models predict that fluid elasticity can cause rheotactic swimmers to accumulate at the center of a microchannel (91). This change in accumulation arises from continuum normal stress differences; whether and how the microstructure fluid structure affects accumulation have not yet been studied.

4. SURFACE ATTACHMENT AND ADHESION

Over 90% of bacteria in the environment live on surfaces. Fluid flows oriented normal or parallel to the surface transport planktonic bacteria to the surface by diffusion or advection, respectively (92), and generate adhesive or frictional forces between bacteria and surfaces (93). Bacteria dynamically or passively approaching surfaces dramatically modify their gene expression to increase production of appendages that drive surface-associated motility behaviors, promoting colonization; small-molecule signals, enabling communication between cells; and extracellular polymers, aiding surface attachment. How bacteria sense surfaces to modify gene expression likely involves one or more mechanical, physical, and chemical cues (94). Here, we describe surface attachment in the presence of flow (**Figure 4**), focusing on near-surface motility behaviors that promote surface attachment and migration.

4.1. Physicochemical Adhesion Models and Their Limitations: A Case Study

In Derjaguin-Landau-Vervey-Overbeek (DLVO) theory, the interaction between a colloidal particle and a surface is modeled as the sum of electrostatic double-layer and van der Waals interactions. DLVO is widely applied to predict interactions between colloids and surfaces in aqueous solutions. Given the size of bacteria, either DLVO or an extended version (xDLVO), which incorporates Lewis acid-base interactions to model hydrophobicity, has been used to predict their initial, non-specific adhesion. Although successful in some settings, these models make assumptions that limit their predictive ability elsewhere (96). They neglect features of bacterial microenvironments, including shear flow, heterogeneities in surface roughness or chemistry, and the 3D geometry of confined porous media. Furthermore, DLVO theories treat the surface of bacteria as smooth and uniform, neglecting passive and active interactions mediated by flagella, pili, and other nanoscale surface structures. DLVO and xDLVO thus constitute a first approximation for predicting adhesion, likely with greater utility for bacteria (such as *S. epidermidis*) bearing few surface appendages.

In flow conditions, additional factors likely influence adhesion. As one example, the distal tip of the type I pili expressed by many species of *E. coli* bears a protein, FimH, able to bind specifically to mannose groups found on the surfaces of the eukaryotic cells that *E. coli* infect. Across an intermediate range of forces, the FimH-mannose bond acts like a catch bond and the bond lifetime is increased (97). As a result, *E. coli* maximally adhere to mannosylated surfaces over

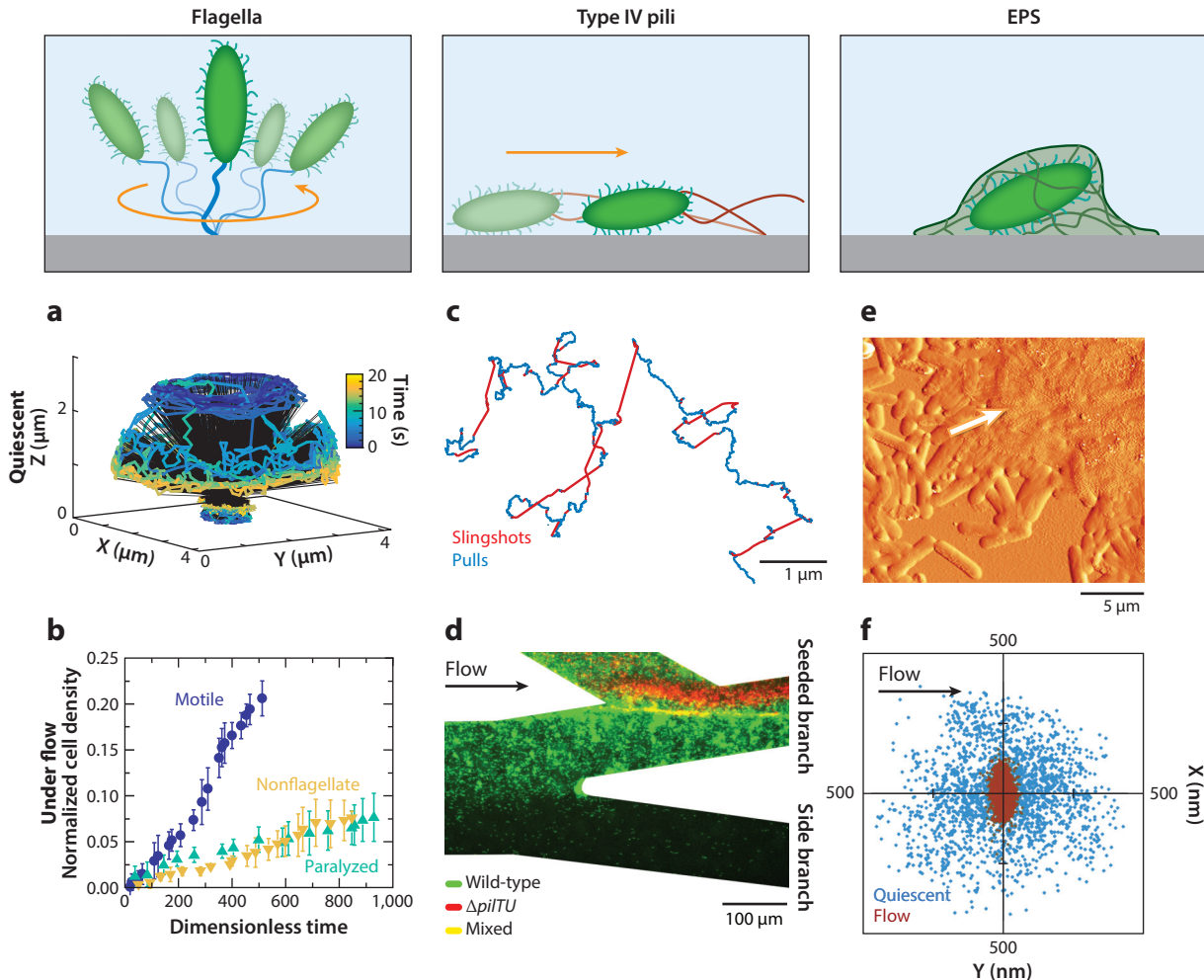


Figure 4

Flow alters near-surface motility and attachment behaviors. (Left column) Rapid spinning of surface-tethered bacteria can strengthen attachment to surfaces under flow. (a) Trajectory of a spinning *Pseudomonas aeruginosa* bacterium (reproduced with permission from Reference 112, copyright 2017 American Chemical Society). (b) Motile *Escherichia coli* bacteria attach to a surface in greater numbers than flagellum-deficient or flagellum-immobilized bacteria when flowed at high rates ($Pe \sim 2 \times 10^4$) (adapted with permission from Reference 104, Copyright 2002 Wiley Periodicals, Inc.). (Middle column) Interactions of flow with asynchronous deployment of type IV pili alter bacterial dispersal. (c) Trajectory of a *P. aeruginosa* bacterium on a polymer brush-coated surface, revealing alternating slow pulls (blue) and rapid slingshots (red), arising from the release of one or more tethered type IV pili (reproduced from Reference 124 and available under the terms of the Creative Commons Attribution 4.0 License). (d) Surface colonization of wild-type (green) and type-IV-pilus-defective (red) *P. aeruginosa* in a branched network. Only wild type dispersed upstream against flow to access the side branch (reproduced with permission from Reference 120, copyright 2015 Elsevier Ltd.). (Right column) Flow can strengthen the attachment of bacteria mediated by extracellular polymeric substances (EPS) (left). (e) Atomic force microscopy image of *Xylella fastidiosa* and its EPS (reproduced from Reference 95 and available under the terms of the Creative Commons Attribution 4.0 License). (f) Position maps of surface-adherent *Staphylococcus salivarius* in quiescent conditions (blue points) and in flow (red points), showing that nanoscale vibrations are reduced under flow (reproduced with permission from Reference 133, copyright 2014 American Chemical Society).

an intermediate range of shear stresses ($\sim 10^{-2}$ to 10^{-1} Pa) (98). Below this range, the bond lifetime is not enhanced; above, the bond instead acts like a slip bond and weakens with increasing stress. The FimH system provides one example of stress-dependent adhesion, linked in this case to a protein. Other stress-dependent mechanisms likely influence bacterial adhesion, as *P. aeruginosa* (99) and type I pili-deficient *E. coli* (100), among others, exhibit stress-enhanced adhesion without a known specific interaction.

4.2. Passive Near-Surface Mobility and Transport

Flows near surfaces may entrain both motile and nonmotile bacteria to promote accumulation. Just as active motility can increase residence times near surfaces (Section 3.1), likewise passive transport-driven mobilities that increase residence times near surfaces increase the probability that bacteria become irreversibly adhered. The FimH adhesin, for example, mediates one near-surface mobility that increases near-surface residence time. In stick-and-roll adhesion, *E. coli* roll over mannose-covered surfaces at velocities of up to $30\text{ }\mu\text{m/s}$ when the shear stress is low but become irreversibly adhered when the shear stress is high ($>0.1\text{ Pa}$) (101). The short-lived bonds formed between FimH and mannose allow cells to travel rapidly along a surface under conditions of low shear stress and accumulate in regions of high shear stress. This mobility may enhance the rate at which *E. coli* colonizes surfaces (102) and may particularly benefit pathogenic bacteria in the high-shear microenvironments near the intestinal surface (101). A second example of passive mobility is sliding mobile adsorption/desorption observed for *S. epidermidis* flowed at a shear rate of $15/\text{s}$ on glass substrates. Movement of bacteria at velocities of $\sim 1\text{ }\mu\text{m/s}$ is attributed to the repulsive interaction between hydrophobic bacteria and hydrophilic substrate (103). A final example of passive mobility is mobile adhesion of *E. coli*, in which type I pili-deficient bacteria move at velocities of 10^{-2} to $10^{-1}\text{ }\mu\text{m/s}$ over surfaces with subnanometric roughness (100). Because the velocities of bacteria in these mobility modes are less than that of the bulk fluid flow, these mobilities cannot be driven solely by hydrodynamic forces but must also involve short-range interactions mediated by surface structures on the bacteria. Moreover, they provide one pathway to increase deposition within zones of relatively high shear, and hence likely alter dispersion in porous media.

4.3. Flagellar Motility and Surface Attachment

Flagella-driven motility, which can promote accumulation of bacteria at surfaces (Section 3), also affects the rate at which bacteria attach. Motile and nonmotile bacteria attach to surfaces at similar rates when the rate of transverse motion set by swimming is comparable to those of passive transport processes such as diffusion (104). Under flow conditions, however, flagellated *E. coli* (104) (**Figure 4b**) and *P. aeruginosa* (105) attach more rapidly to surfaces than bacteria lacking flagella. The mechanisms by which flagella enhance attachment likely depend on the dominant transport mechanism, ranging from upstream swimming when the rate of advection is somewhat less than passive diffusion ($\text{Pe} \sim 0.1$) (105) to attachment strengthened by flagellar rotation in the opposite limit ($\text{Pe} \sim 2 \times 10^4$) (104). These mechanisms allow motile swimming bacteria to idle near surfaces, increasing their retention and dispersion within a 3D porous medium (77). Enhanced dispersion occurs only when the rate at which bacteria swim toward the surface exceeds the rate at which they are advected through the porous medium. Because surface attachment also involves short-range interactions, however, different strains of bacteria may exhibit other behaviors. As one example, swimming motility of the soil bacterium *Azotobacter vinelandii* reduces attachment in model 2D glass micropillar arrays (106). Thus, specific physicochemical interactions may still alter attachment processes even when the dominant transport process is the same.

Beyond modifying transverse transport, bacteria use flagella in other ways near a surface to promote or reduce attachment. *E. coli* bacteria, for example, better adhere to surfaces featuring microscale trenches when their flagella are free to rotate (107). When attached to a surface by a flagellum, bacteria can still rotate the flagellar motor and thus spin rapidly on the surface at rates of ~ 2.5 Hz for *E. coli* (108) and ~ 5 Hz for *P. aeruginosa* (109). The spinning behavior of tethered bacteria reflects both hydrodynamic (110) and physicochemical (111) interactions of bacteria with the surface. Moreover, spinning can help bacteria detach from surfaces (109, 111). A detailed hydrodynamic comparison of spinning *P. aeruginosa*, the metal-reducing bacterium *Shewanella oneidensis*, and the cholera pathogen *Vibrio cholerae* reveals that the mechanical properties of the flagellum, its interaction with the surface, and the shape of the bacterium determine the likelihood of detachment (110). Finally, flagellar spinning generates other near-surface motilities, such as lateral diffusive spinning in *P. aeruginosa* (112) (Figure 4a). Although these motility modes reflect hydrodynamic interactions with nearby surfaces, how flow alters these motilities remains largely uninvestigated.

4.4. Type IV Pili-Mediated Dispersal and Adhesion in Flow

Bacteria that live on surfaces express several types of pili. Type I pili, distributed uniformly around the cell surface, help bacteria attach to surfaces (Section 4.1). Type IV pili, located preferentially at the poles of a bacterium, aid in attachment and moreover enable collective surface motility modes. Bacteria such as *P. aeruginosa* and the gonorrhreal pathogen *Neisseria gonorrhoeae* twitch by repeatedly extending and retracting type IV pili to propel forward on a surface (113). Although type IV pili can actuate motion only on surfaces, their presence nonetheless modifies patterns of swimming motility. Near glass surfaces, swimming *V. cholerae* exhibit meandering roaming trajectories and highly curved orbiting trajectories with longer residence times arising from frictional interactions between the type IV pili and the surface. Only orbiting cells are able to irreversibly attach (114). Similarly, interactions between the type IV pili of *P. aeruginosa* and host cell surfaces, likely mediated by transient receptor-ligand interactions, increase the number of highly curved and low-speed trajectories suggestive of close contact (115). Hence, both nonspecific and specific type IV pili-mediated interactions modify swimming behaviors for bacteria.

Individual bacteria can use type IV pili to walk with short directional persistence (~ 2 μm) when oriented perpendicular to the surface and crawl with longer directional persistence (~ 6 μm) when oriented parallel to the surface (116). Differences between the directional persistence of walking and crawling lead to diffusive and superdiffusive surface motion, respectively, enabling efficient coverage of area and linear distance (109). In the presence of shear flow, bacteria can crawl on surfaces against the flow direction using type IV pili. This upstream twitching, observed for *P. aeruginosa* (117) and the plant pathogens *Xylella fastidiosa* (118) and *Acidovorax citrulli* (119), is similar to the upstream rheotaxis observed for swimming bacteria in that it originates from interactions between appendage-driven motion and flow. Upstream twitching, though, requires type IV pili and a nearby surface. Bacteria tethered asymmetrically at one pole by type IV pili are dragged by shear flow to align along the flow direction. To twitch upstream, bacteria retract the type IV pili at the tethered pole (117). Upstream twitching has pronounced consequences for the ability of bacteria to explore confined microchannel networks: *P. aeruginosa* bacteria possessing type IV pili can fully explore side branches of a network, whereas bacteria lacking pili remain localized to the linear channel in which they are seeded (120) (Figure 4d). This unusual dispersal pattern arises from the combination of zig-zag slingshot motions by the bacteria (121) with shear-flow-driven detachment and downstream reattachment. By combining slingshots and reattachment events, bacteria can diffuse in the direction lateral to flow while counter-advection

Extracellular polymeric substances (EPSs): biopolymers that make up the biofilm matrix, consisting primarily of polysaccharides but also including proteins, glycoproteins and glycolipids, and/or extracellular DNA

against the flow direction (120). This flow-altered motility pattern gives bacteria an advantage to colonize highly branched networks, such as the microvasculature.

Finally, bacteria can use type IV pili to move on rough or soft surfaces. Even modest topographic features can confine bacteria, with barriers as short as 1 μm in height able to trap twitching *Myxococcus xanthus* or *N. gonorrhoeae* bacteria within grooves (122). Similarly, bacteria modify type IV pili–driven motility when moving on viscoelastic surfaces of varying fluidity or compliance. For example, *N. gonorrhoeae* bacteria twitch increasingly slowly on supported lipid membranes as the fluidity of the membrane is increased, so much so that they become effectively confined on nonfluid islands patterned within the fluid membrane (123). Likewise, bacteria using type IV pili slingshot more frequently on softer polymer brush surfaces (124) (Figure 4c). In slingshot motility, bacteria alternate slow linear translation (0.03 $\mu\text{m/s}$) with a fast rotation-translation (1 $\mu\text{m/s}$) (121). The more frequent rapid motions on soft surfaces exploit the shear-thinning rheology of the polymers to reduce the energy dissipated during twitching on a soft surface. These examples are consistent with recent studies indicating that type IV pili may act as mechanosensors for bacteria, sensing both solid surface contact (125) as well as fluid shear (126), and are consistent with the idea that very soft surfaces may hinder biofilm formation (126). Indeed, in the extreme soft limit, liquid-infused surfaces frustrate bacterial attachment (127).

4.5. Extracellular Polymers Promote Attachment and Colonization in Flow

As a precursor to adhesion, bacteria near surfaces produce extracellular polymeric substances (EPSs). In aqueous solution at dilute concentrations [$\sim 3 \times 10^{17}$ chains/L (128)], the EPS forms a weak network with viscoelasticity dominated by polymer entanglements and divalent ion–mediated intermolecular associations (129). EPS expression alters bacterial surface motility. For example, *P. aeruginosa* that crawl across a surface using type IV pili excrete EPS trails that other bacteria follow to explore surfaces (130). EPS molecules can also alter the adhesive behavior of individual bacteria deposited from flow onto flat surfaces (131) and within porous media (132). Beyond the changes in adhesion arising from physicochemical effects such as steric repulsion and DLVO-type interactions, flow-induced deformation of the EPS itself can also affect bacterial adhesion. Staphylococcal bacteria adhering to a surface vibrate due to Brownian motion, with an amplitude that characterizes the softness of their EPS layer. Shear flow at a rate of 10/s reversibly deforms and stiffens the surrounding EPS, leading to smaller vibrational amplitudes in the direction normal to flow than perpendicular to it (133) (Figure 4f). Hence, flow-induced deformation of the polymers that mediate attachment (EPS, but also polymeric nanofibers such as flagella and pili) can modify the strength of adhesion.

4.6. Shape-Enhanced Attachment in Flow

Although the previous examples focus on interactions mediated by surface polymers in flow, other physical parameters, such as shape, affect the likelihood that bacteria adhere to surfaces. First, bacteria of greater shape anisotropy (length/width) are preferentially retained when flowed through a dense packed bed, whereas bacteria in the effluent are smaller and rounder (134). This result, obtained across a variety of environmental isolates, suggests a generic role of geometry: Anisotropic bacteria have a larger capture cross-section than spherical bacteria of similar volume when flowed through a tortuous porous medium featuring curved streamlines. Hence, this purely geometric effect should also operate for colloids and nonmotile bacteria. Second, flow enhances surface adhesion for *C. crescentus*, shaped like a curved rod, over its straight-rod mutants (135). *C. crescentus* attaches to a surface using a strongly adhesive holdfast and expresses flagella and

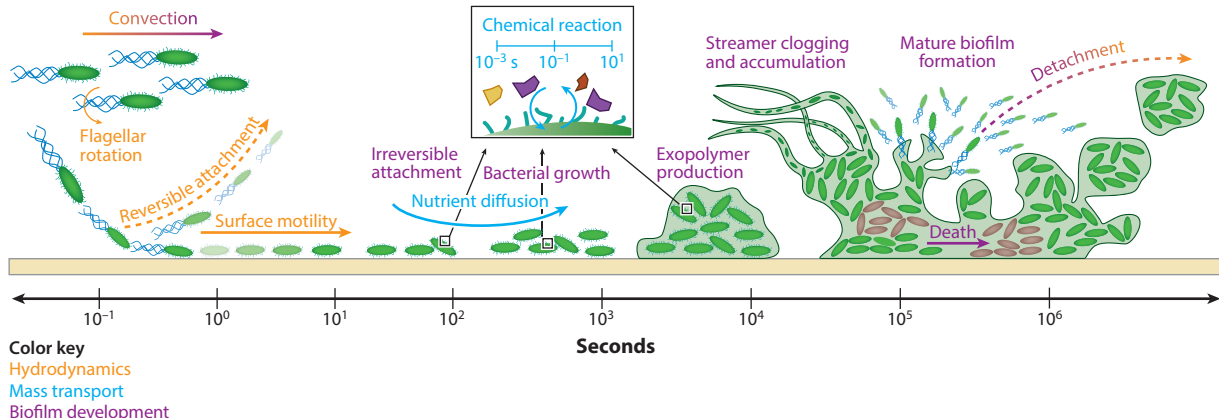


Figure 5

Relevant timescales for the growth of bacterial biofilms. Processes underlying biofilm growth can be sorted into one of three categories (adapted with permission from 136): hydrodynamics (orange), mass transport (blue), and biofilm development (purple). Hydrodynamic processes typically occur over timescales of 10^{-1} – 10^1 s; mass transport over 10^{-3} – 10^1 s (chemical reactions) and 10^1 – 10^3 s (nutrient diffusion); and biofilm growth, decay, and detachment over 10^4 – 10^7 s. Processes generally occur over the indicated timescales but may occur continuously, contemporaneously, and over a wide range of timescales.

pili at its other pole. In the moderate flow environments (wall shear stresses less than ~ 2 Pa) characteristic of its native freshwater habitats, flow orients curved *C. crescentus* to arc over the surface; after the bacterium divides, this orientation reduces the distance between the surface and the polar pili, which promote adhesion, on the new daughter cell (135). This advantage afforded by curved shape, however, is lost in stronger flows (135). Environmental flows may thus apply a selective pressure on properties that increase surface attachment of bacteria in their native habitats.

5. BIOFILMS

Biofilm formation is dynamic, occurring over a wide range of timescales (Figure 5) set by concurrent hydrodynamics, mass transport, and biofilm growth processes (136). Hydrodynamic processes occur on short timescales, as bacteria move through surrounding fluids and interact with nearby surfaces. Chemical reactions occur on short and intermediate timescales, driven by transport of nutrients and signals. In turn, nutrient transport and reactions facilitate growth of bacteria and production of exopolymers. Mature biofilms grow and then decay, influenced by fluid flows that transport nutrients but reshape and erode biofilm structures. Here, we describe how biofilm structure is shaped by and in turn constrains fluid flow and chemical transport.

5.1. Fluid Shear Alters Biofilm Structure

Fluid flow near surfaces generates shear stresses that affect the formation and structure of biofilms in at least three ways. First, shear flow can enhance biofilm formation. Physiologically relevant shear stresses of order 10^{-2} – 10^0 Pa can trigger the expression of EPS constituents, such as polysaccharide intracellular adhesin in *S. epidermidis* (137). Shear forces of only 0.002 pN [orders of magnitude lower than the ~ 100 -pN forces (138) exerted by type IV pili during retraction] boost expression of molecules important for signal transduction and biofilm formation, such as 3',5'-cyclic diguanylic acid in *P. aeruginosa* (126). Fluid shear thus generates a positive feedback loop, initiating biofilm formation that leads to larger frictional forces and thus increases EPS production.

Second, flow can affect the structure and mechanics of biofilms. Mechanically, biofilms behave like soft viscoelastic solids, with a low elastic modulus [$<10^4$ Pa (139)], a long relaxation time [$\sim 10^3$ s, likely reflecting the shortest time period over which a biofilm can change its phenotype in response to a transient mechanical stress (140)], and a finite yield stress [~ 10 Pa (141)]. Their structural and mechanical response to shear is thus time and rate dependent. When first exposed to fluid shear, biofilms compress and decrease in thickness (142). Biofilms grown under shear often contain more bacteria (143) and a denser EPS matrix (144) but exhibit a wide variation in mechanical properties across the range of growth stresses probed in experiment. Whereas biofilms of *P. aeruginosa* (145) and sulfate-reducing *Desulfovibrio* (146) are more rigid when grown under higher shear stress ($0.9 \rightarrow 5.3$ N/m 2), biofilms of the oral bacterium *Streptococcus oralis* have decreased compressive strength and elastic modulus ($0.027 \rightarrow 1.0$ N/m 2), and biofilms of the oral bacterium *Actinomyces naeslundii* exhibit no significant changes in mechanical properties ($0.0001 \rightarrow 0.05$ N/m 2) (147).

Finally, shear flow can remove cells, clusters, and biofilms from surfaces. Hydrodynamic interactions between biofilms and the externally imposed fluid flow can generate recirculating eddies that lead to forces perpendicular to the biofilm interface, even under laminar flow conditions (16). The combination of normal and shear forces leads to the detachment and removal of biofilm particles or clusters (136) as well as whole biofilms (148). The dominant detachment mechanism, however, depends on the rate of change of the fluid shear stress as well as its magnitude (149) and may reflect contributions from cohesive bonds within the biofilm and adhesive bonds between the biofilm and the surface (150). After detaching from the main biofilm, clusters can roll slowly along the surface, dragged along by the shear flow and slowed by forming transient surface-attached tethers (151), reminiscent of the shear-strengthened (molecular) FimH-mannose catch bonds formed by *E. coli*.

5.2. Confined Flow Alters Biofilm Structure

Biofilms grown in fluid flow, whether turbulent (high Re) streams or laminar (low Re) microchannels, flow cells, and membranes, can feature extended filamentous structures termed streamers. In microscale channels, biofilm streamers of width $\sim 10\text{--}20$ μm (152) can approach aspect ratios of at least 10 (153). These structures are observed in a wide variety of biofilm-forming bacteria, including *P. aeruginosa* (154), *Staphylococcus aureus* (155), *S. epidermidis* (137), and *E. coli* (156). Streamers form in regions of high fluid shear [$\sim 1/\text{s}$ (157)] because biofilms behave rheologically like Bingham solids, undergoing nonlinear plastic flow only above a critical shear stress (150). Although often formed under turbulent conditions in environmental settings, in laminar flow they can form in curved channels by accumulation of biomass in recirculating flows (157) or in porous media by surface capture of flocs (158). Shear flow subsequently extends the biomass into a slender filament. Streamers tethered at the corners of channels can cross fluid streamlines to bridge across channels (152), acting as hinged filaments that reorient in flow (155). Practically, streamers underpin one mechanism of catastrophic clogging: Detached EPS is captured on streamers, clogging the channel on timescales (~ 30 min) much shorter than those required for growth (~ 6.5 h) (159).

Other confining geometries can shape biofilms that develop under flow. Formation of *S. oneidensis* biofilms near 2D baffle structures depends on both fluid velocity and baffle spacing (160). When advective transport occurs on similar timescales to microbial motility, bacteria can penetrate baffles and form biofilms in the semiconfined space between them; when the flow rate is increased, advective transport dominates, and biofilm formation is limited to the areas accessible by the fluid streamlines. Increasing the baffle spacing, however, generates secondary flows that enable bacteria to enter the semiconfined space and form biofilms (160). Although the confining

length scale ($\sim 100 \mu\text{m}$) is much larger than the size of a bacterium, the relative motility imparted by flow and by bacterial motility controls biofilm formation within the confined regions.

5.3. Biofilm Growth Modifies Confined Flow

Just as fluid flow and shear influence how biofilms form and mature, biofilms likewise alter fluid flow through confined media. Biofilms can grow to fill pores and occlude flows or decay, lyse, and detach to open new flow channels (161). These changes in fluid flow alter macroscopic transport of fluid and nutrients, leading to a complex feedback loop for biofilm growth and decay in porous media.

Combined experiments and simulations of flow through a 3D packed bed ($\text{Re} = 0.1\text{--}10$) reveal that biofilm growth reduces the conductivity of the fluid and increases the number of dead-end pores (162). Simulations coupling biomass growth to nutrient use suggest that biofilm growth preferentially occurs away from the main flow path, in narrow channels normal to the flow direction, and is not limited by nutrient transport (162). Conversely, experiments and models in 2D microfluidic networks at low Re suggest a critical role for nutrient transport for multispecies biofilms (163). Rapid growth of a biofilm in a narrow channel can clog the channel and reduce fluid transport there, while redirecting flow to other channels. A model incorporating biofilm growth and flow-induced detachment suggests that strong flow (when detachment exceeds growth) favors faster-growing biofilms, but weak flow favors slow-growing biofilms (163). A final example of biofilm growth in confined flow arises when strains that can and cannot produce EPS compete to form biofilms. A matrix-producing wild-type (WT) *P. aeruginosa* strain outcompetes a mutant strain that is deficient in producing EPS (and hence is detached by gentle shear) to form biofilms on flat surfaces within microfluidic channels (164). In microfluidic channels containing irregularly spaced and sized posts, however, both the matrix-producing WT and the non-EPS-producing mutant are able to form biofilms. The growth of WT biofilm occludes pores and generates regions of low fluid shear in which the EPS-deficient mutant can attach and form biofilms. These studies highlight different ways by which confined flow and biofilm growth repeatedly interact to modify pore structure and connectivity, with the properties of different groups of bacteria molding the local structure and composition of biofilms.

Quorum sensing (QS):

process by which bacteria communicate through small-molecule signals to coordinate production of extracellular factors

Autoinducer:

diffusible small molecule that regulates production of a variety of chemical signals and whose uptake leads to an increase in its production, thereby generating a positive feedback loop

5.4. Flow-Altered Transport in and near Biofilms: Example of Quorum Sensing

Living bacteria within a biofilm must access nutrients and chemical signals necessary for sustenance and communication; conversely, strategies to eradicate biofilms require transport of dispersants to cells sheltered within. The tortuous and porous biofilm structure, consisting of dense cell clusters as well as channels and voids, hinders small molecule transport. Within dense cell clusters, transport of small molecules is dominated by diffusion (165), but both advection and diffusion can transport molecules within larger voids or channels. Mass transport within a biofilm thus resembles that in a porous medium (166). Biofilms grown in flow are shaped by their need both for efficient mass transfer and to resist erosion by shear stress, such that their effective diffusivity decreases towards the biofilm base (167). How biofilms respond to nutrient transport, however, may be surprisingly complex: Both low and high nutrient concentrations can trigger the release of cells from biofilms to search for more favorable environments or better access the local nutrients, respectively (168).

Transport of chemical signals is of special interest for quorum sensing (QS), required by many bacteria species to initiate multicellular behaviors. Bacteria detect and respond to autoinducers produced by themselves and by other bacteria, enabling communication between cells (169). Autoinducers are transported between cells and trigger QS only upon exceeding a critical concentration. Hence, QS is affected by the population size and density as well as the local mass-transfer

environment, demonstrated by confining *P. aeruginosa* bacteria in small ($\sim 10\text{-}\mu\text{m}$)³ 3D traps that are permeable to fluid flow (170) or by varying the level of water saturation on leaves harboring the plant pathogen *Pseudomonas syringae* (171). Tortuous geometries impose constraints on the onset of QS and quorum size that reflect a balance between accessing nutrients and retaining autoinducers in flow (172). Although the term quorum sensing suggests that a critical cell number must be exceeded, an individual bacterium confined within a small ($\sim 10\text{-}\mu\text{m}$)³, isolated, impermeable fluid environment can generate a sufficient autoinducer density to trigger QS (173, 174)—useful for a soil bacterium trapped in a pore, or for an isolated pathogen. These examples show that both confinement and flow alter QS, as expected for bacteria living in complex geometries permeated by fluid flow.

Although most studies of QS have been performed in planktonic cultures, biofilms can also contain cells at sufficiently high number and/or density to activate QS. Because QS systems regulate key aspects of biofilm formation for many bacteria, understanding how flow modifies QS within biofilms has significant implications for biofilm maturation and dispersal. Similar to how it modifies nutrient transport and convective flow, the biofilm matrix is expected to alter QS by modifying autoinducer transport. In *P. aeruginosa*, for which QS promotes biofilm formation, increasing the fluid flow rate ($Re = 0.3 \rightarrow 300$, $Pe = 700 \rightarrow 70,000$) increases the amount of biofilm biomass required to initiate QS; at an even higher flow rate ($Re = 3,000$, $Pe = 7,000,000$) QS is never fully induced (175), and the morphology of WT and QS-deficient biofilms is similar (148). Flow-driven changes in QS expression can have pronounced consequences for biofilm formation in confined flow. In *S. aureus*, even gentle fluid flow ($Re \sim 10^{-3}$, $Pe \sim 30$) generates spatial gradients of QS expression. Near the biofilm periphery, efficient advection of autoinducers represses QS; within the biofilm, autoinducer concentration builds over time to active QS (176). Further, when biofilm formation is repressed by QS, flow within a microchannel leads to spatially heterogeneous biofilms by increasing the autoinducer concentration downstream (176). Different species of bacteria exhibit distinct responses to QS; how flow affects QS within biofilms for a given species of bacteria depends on the production of the sheltering extracellular matrix (177) and, likely, its ability to resist deformation under flow (178). Hence, QS-directed processes, such as biofilm formation and dispersal, are expected to be nonuniform along extended or tortuous flow pathways, and among the multispecies communities encountered in practical applications such as membrane or pipeline fouling.

SUMMARY POINTS

1. Fluid flow within confined geometries modifies how bacteria swim, attach to surfaces, and form biofilms. Whether beneficial or deleterious, how flow and confinement affect these phenomena must be considered when designing or operating processes involving bacteria.
2. For planktonic swimming bacteria, nearby surfaces introduce steric interactions that couple with Newtonian and non-Newtonian fluid hydrodynamics and shear to generate curved trajectories, promote or reduce near-surface accumulation, induce rheotaxis, and lead to collective self-organized motility patterns.
3. Although species and system dependent, flow generally promotes bacterial adhesion to surfaces by strengthening catch bonds and increasing near-surface residence time and can introduce new mobility modes such as upstream twitching, which enhance their ability to rapidly spread on surfaces.

4. The hydrodynamic stress imposed by externally driven flows leads to complex changes in the structure, mechanical properties, and growth of biofilms, which may in turn modify flow fields in porous materials. Flowing within and around a biofilm, fluids can transport nutrients and chemical signals that alter the growth rate, dispersion, and quorum-sensing capabilities of biofilms.

FUTURE ISSUES

1. Although research efforts have largely focused on solid/liquid interfaces, liquid/liquid and gas/liquid interfaces are common in natural and engineered processes, such as oil droplets after an oil spill or bubbles in sparged bioreactors. How bacteria attach to, transport along, and interact with these interfaces is not well understood.
2. Whereas most microfluidic and engineering environments are well ordered or periodic, environmental settings are often random and commonly possess a wide distribution of length scales. Understanding how transport, attachment, and growth of bacteria and biofilms are modified by medium geometry will inform applications from membrane fouling to microbially enhanced oil recovery.
3. This review focuses largely on the effect of steady-state confined flow, which already presents a rich and complex scientific problem. In many engineering processes and environmental systems, however, flow fluctuates over time. Transient flow conditions, only beginning to be studied, will likely further affect bacterial behavior near surfaces and in confinement.
4. Outside the lab, bacteria species rarely exist in isolation. How flow shapes interactions between the different species in a spatially defined consortium must be considered when designing and developing engineering solutions.
5. Controlling bacterial behavior near surfaces and in flow is fundamentally complex. Engineers may apply microbiological approaches, modifying the bacterial genome and targeting the epigenetic response, or physical approaches, developing materials and devising processing routes informed by relevant physical regimes of mass and momentum transport. Robust and effective solutions will require integrating both of these approaches.

DISCLOSURE STATEMENT

The authors are not aware of any affiliations, memberships, funding, or financial holdings that might be perceived as affecting the objectivity of this review.

ACKNOWLEDGMENTS

This research was made possible in part by a grant from The Gulf of Mexico Research Initiative, and in part by grants from the National Science Foundation (DMR-1151133) and the Welch Foundation (E-1869).

LITERATURE CITED

1. Baeshen NA, Baeshen MN, Sheikh A, Bora RS, Ahmed MMM, et al. 2014. Cell factories for insulin production. *Microb. Cell Fact.* 13:141

2. Sanchez-Garcia L, Martín L, Mangues R, Ferrer-Miralles N, Vázquez E, Villaverde A. 2016. Recombinant pharmaceuticals from microbial cells: a 2015 update. *Microb. Cell Fact.* 15:33
3. Hammes F, Egli T. 2010. Cytometric methods for measuring bacteria in water: advantages, pitfalls and applications. *Anal. Bioanal. Chem.* 397:1083–95
4. Hegab HM, ElMekawy A, Stakenborg T. 2013. Review of microfluidic microbioreactor technology for high-throughput submerged microbiological cultivation. *Biomicrofluidics* 7:1–14
5. Tuson HH, Weibel DB. 2013. Bacteria-surface interactions. *Soft Matter* 9:4368–80
6. Fernandes R, Zuniga M, Sassine FR, Karakoy M, Gracias DH. 2011. Enabling cargo-carrying bacteria via surface attachment and triggered release. *Small* 7:588–92
7. Rozhok S, Shen CF, Littler PL, Fan Z, Liu C, et al. 2005. Methods for fabricating microarrays of motile bacteria. *Small* 1:445–51
8. Hochbaum AI, Aizenberg J. 2010. Bacteria pattern spontaneously on periodic nanostructure arrays. *Nano Lett.* 10:3717–21
9. Mee MT, Wang HH. 2012. Engineering ecosystems and synthetic ecologies. *Mol. BioSyst.* 8:2470–83
10. Schinner T, Letzner A, Liedtke S, Castro FD, Eydelnant IA, Tufenkji N. 2010. Transport of selected bacterial pathogens in agricultural soil and quartz sand. *Water Res.* 44:1182–92
11. Ribet D, Cossart P. 2015. How bacterial pathogens colonize their hosts and invade deeper tissues. *Microbes Infect.* 17:173–83
12. Sahari A, Traore MA, Scharf BE, Behkam B. 2014. Directed transport of bacteria-based drug delivery vehicles: Bacterial chemotaxis dominates particle shape. *Biomed. Microdevices* 16:717–25
13. Guasto JS, Rusconi R, Stocker R. 2012. Fluid mechanics of planktonic microorganisms. *Annu. Rev. Fluid Mech.* 44:373–400
14. Rusconi R, Stocker R. 2015. Microbes in flow. *Curr. Opin. Microbiol.* 25:1–8
15. Lauga E. 2016. Bacterial hydrodynamics. *Annu. Rev. Fluid Mech.* 48:105–30
16. Stewart PS. 2012. Mini-review: convection around biofilms. *Biofouling* 28:187–98
17. Persat A, Nadell CD, Kim MK, Ingremeau F, Siryaporn A, et al. 2015. The mechanical world of bacteria. *Cell* 161:988–97
18. Wessel AK, Hmelo L, Parsek MR, Whiteley M. 2013. Going local: technologies for exploring bacterial microenvironments. *Nat. Rev. Microbiol.* 11:337–48
19. Frank M, Anderson D, Weeks ER, Morris JF. 2003. Particle migration in pressure-driven flow of a Brownian suspension. *J. Fluid Mech.* 493:363–78
20. Morris JF, Brady JF. 1998. Pressure-driven flow of a suspension: buoyancy effects. *Int. J. Multiphase Flow* 24:105–30
21. Pandey R, Conrad JC. 2012. Effects of attraction strength on microchannel flow of colloid-polymer depletion mixtures. *Soft Matter* 8:10695–703
22. Nikoubashman A, Mahynski NA, Pirayandeh AH, Panagiotopoulos AZ. 2014. Flow-induced demixing of polymer-colloid mixtures in microfluidic channels. *J. Chem. Phys.* 140:094903
23. Huang LR, Cox EC, Austin RH, Sturm JC. 2004. Continuous particle separation through deterministic lateral displacement. *Science* 304:987–90
24. He K, Retterer ST, Srijanto BR, Conrad JC, Krishnamoorti R. 2014. Transport and dispersion of nanoparticles in periodic nanopost arrays. *ACS Nano* 8:4221–27
25. Auset M, Keller AA. 2004. Pore-scale processes that control dispersion of colloids in saturated porous media. *Water Resour. Res.* 40:W03503
26. Bales R, Gerba C, Grondin G, Jensen S. 1989. Bacteriophage transport in sandy soil and fractured tuff. *Appl. Environ. Microbiol.* 55:2061–67
27. Mason TG, Weitz DA. 1995. Optical measurements of frequency-dependent linear viscoelastic moduli of complex fluids. *Phys. Rev. Lett.* 74:1250–53
28. Cai LH, Panyukov S, Rubinstein M. 2011. Mobility of nonsticky nanoparticles in polymer liquids. *Macromolecules* 44:7853–63
29. Poling-Skutvik R, Krishnamoorti R, Conrad JC. 2015. Size-dependent dynamics of nanoparticles in unentangled polyelectrolyte solutions. *ACS Macro Lett.* 4:1169–73
30. Berry H, Chaté H. 2014. Anomalous diffusion due to hindering by mobile obstacles undergoing Brownian motion or Orstein-Uhlenbeck processes. *Phys. Rev. E* 89:022708

31. Babayekhorasani F, Dunstan DE, Krishnamoorti R, Conrad JC. 2016. Nanoparticle diffusion in crowded and confined media. *Soft Matter* 12:8407–16
32. Scholz C, Wirner F, Gomez-Solano JR, Bechinger C. 2014. Enhanced dispersion by elastic turbulence in porous media. *EPL* 107:054003
33. Jacob JDC, Krishnamoorti R, Conrad JC. 2017. Particle dispersion in porous media: differentiating effects of fluid rheology and geometry. *Phys. Rev. E* 96:022610
34. Babayekhorasani F, Dunstan DE, Krishnamoorti R, Conrad JC. 2016. Nanoparticle dispersion in disordered porous media with and without polymer additives. *Soft Matter* 12:5676–83
35. Purcell EM. 1977. Life at low Reynolds number. *Am. J. Phys.* 45:3–11
36. Misselwitz B, Barrett N, Kreibich S, Vonaesch P, Andritschke D, et al. 2012. Near surface swimming of *Salmonella* Typhimurium explains target-site selection and cooperative invasion. *PLOS Pathog.* 8:e1002810
37. Lane MC, Lockatell V, Monterosso G, Lamphier D, Weinert J, et al. 2005. Role of motility in the colonization of uropathogenic *Escherichia coli* in the urinary tract. *Infect. Immun.* 73:7644–56
38. Yawata Y, Nguyen J, Stocker R, Rusconi R. 2016. Microfluidic studies of biofilm formation in dynamic environments. *J. Bacteriol.* 198:2589–95
39. Lauga E, Powers TR. 2009. The hydrodynamics of swimming microorganisms. *Rep. Prog. Phys.* 72:096601
40. Frymier PD, Ford RM, Berg HC, Cummings PT. 1995. Three-dimensional tracking of motile bacteria near a solid planar surface. *PNAS* 92:6195–99
41. Lauga E, DiLuzio WR, Whitesides GM, Stone HA. 2006. Swimming in circles: motion of bacteria near solid boundaries. *Biophys. J.* 90:400–12
42. DiLuzio WR, Turner L, Mayer M, Garstecki P, Weibel DB, et al. 2005. *Escherichia coli* swim on the right hand side. *Nature* 435:1271–74
43. Di Leonardo R, Dell'Arciprete D, Angelani L, Iebba V. 2011. Swimming with an image. *Phys. Rev. Lett.* 106:038101
44. Hu J, Wysocki A, Winkler RG, Gompper G. 2015. Physical sensing of surface properties by microswimmers directing bacterial motion via wall slip. *Sci. Rep.* 5:9586
45. Lemelle L, Palierne JF, Chatre E, Vaillant C, Place C. 2013. Curvature reversal of the circular motion of swimming bacteria probes for slip at solid/liquid interfaces. *Soft Matter* 9:9759–62
46. Berke AP, Turner L, Berg HC, Lauga E. 2008. Hydrodynamic attraction of swimming microorganisms by surfaces. *Phys. Rev. Lett.* 101:038102
47. Li G, Bensson J, Nisimova L, Munger D, Mahautmr P, et al. 2011. Accumulation of swimming bacteria near a solid surface. *Phys. Rev. E* 84:041932
48. Vigeant MAS, Ford RM, Wagner M, Tamm LK. 2002. Reversible and irreversible adhesion of motile *Escherichia coli* cells analyzed by total internal reflection aqueous fluorescence microscopy. *Appl. Environ. Microbiol.* 68:2794–801
49. Hernandez-Ortiz JP, Stoltz CG, Graham MD. 2005. Transport and collective dynamics in suspensions of confined swimming particles. *Phys. Rev. Lett.* 95:204501
50. Drescher K, Dunkel J, Cisneros LH, Ganguly S, Goldstein RE. 2011. Fluid dynamics and noise in bacterial cell-cell and cell-surface scattering. *PNAS* 108:10940–45
51. Li G, Tang JX. 2009. Accumulation of microswimmers near a surface mediated by collision and rotational Brownian motion. *Phys. Rev. Lett.* 103:078101
52. Li G, Tam LK, Tang JX. 2008. Amplified effect of Brownian motion in bacterial near-surface swimming. *PNAS* 105:18355–59
53. Bianchi S, Saglimbeni F, Di Leonardo R. 2017. Holographic imaging reveals the mechanism of wall entrapment in swimming bacteria. *Phys. Rev. X* 7:011010
54. Spagnolie SE, Lauga E. 2012. Hydrodynamics of self-propulsion near a boundary: predictions and accuracy of far-field approximations. *J. Fluid Mech.* 700:105147
55. Sipos O, Nagy K, Di Leonardo R, Galajda P. 2015. Hydrodynamic trapping of swimming bacteria by convex walls. *Phys. Rev. Lett.* 114:258104
56. Kaya T, Koser H. 2009. Characterization of hydrodynamic surface interactions of *Escherichia coli* cell bodies in shear flow. *Phys. Rev. Lett.* 103:138103

57. Jeffery GB. 1922. The motion of ellipsoidal particles immersed in a viscous fluid. *Proc. R. Soc. Lond. A* 102:161–79
58. Kaya T, Koser H. 2012. Direct upstream motility in *Escherichia coli*. *Biophys. J.* 102:1514–23
59. Marcos, Fu HC, Powers TR, Stocker R. 2012. Bacterial rheotaxis. *PNAS* 109:4780–85
60. Hill J, Kalkanci O, McMurry JL, Koser H. 2007. Hydrodynamic surface interactions enable *Escherichia coli* to seek efficient routes to swim upstream. *Phys. Rev. Lett.* 98:068101
61. Figueroa-Morales N, Miño G, Rivera A, Caballero R, Clément E, et al. 2015. Living on the edge: transfer and traffic of *E. coli* in a confined flow. *Soft Matter* 11:6284–93
62. Costanzo A, Di Leonardo R, Ruocco G, Angelani L. 2012. Transport of self-propelling bacteria in micro-channel flow. *J. Phys. Condens. Matter* 24:065101
63. Molaei M, Barry M, Stocker R, Sheng J. 2014. Failed escape: Solid surfaces prevent tumbling of *Escherichia coli*. *Phys. Rev. Lett.* 113:068103
64. Molaei M, Sheng J. 2016. Succeed escape: Flow shear promotes tumbling of *Escherichia coli* near a solid surface. *Sci. Rep.* 6:35290
65. Mathijssen AJTM, Doostmohammadi A, Yeomans JM, Shendruk TN. 2016. Hotspots of boundary accumulation: dynamics and statistics of micro-swimmers in flowing films. *J. R. Soc. Interface* 13:20150936
66. Rusconi R, Guasto JS, Stocker R. 2014. Bacterial transport suppressed by fluid shear. *Nat. Phys.* 10:212–17
67. Sokolov A, Aranson IS. 2012. Physical properties of collective motion in suspensions of bacteria. *Phys. Rev. Lett.* 109:248109
68. López HM, Gachelin J, Douarche C, Auradou H, Clément E. 2015. Turning bacteria suspensions into superfluids. *Phys. Rev. Lett.* 115:028301
69. Sokolov A, Apodaca MM, Grzybowski BA, Aranson IS. 2010. Swimming bacteria power microscopic gears. *PNAS* 107:969–74
70. Kaiser A, Peshkov A, Sokolov A, Ten Hagen B, Löwen H, Aranson IS. 2014. Transport powered by bacterial turbulence. *Phys. Rev. Lett.* 112:158101
71. Hernandez-Ortiz JP, Underhill PT, Graham MD. 2009. Dynamics of confined suspensions of swimming particles. *J. Phys. Condens. Matter* 21:204107
72. Dombrowski C, Cisneros L, Chatkaew S, Goldstein RE, Kessler JO. 2004. Self-concentration and large-scale coherence in bacterial dynamics. *Phys. Rev. Lett.* 93:098103
73. Wioland H, Woodhouse FG, Dunkel J, Kessler JO, Goldstein RE. 2013. Confinement stabilizes a bacterial suspension into a spiral vortex. *Phys. Rev. Lett.* 110:268102
74. Lushi E, Wioland H, Goldstein RE. 2014. Fluid flows created by swimming bacteria drive self-organization in confined suspensions. *PNAS* 111:9733–38
75. Wioland H, Lushi E, Goldstein RE. 2016. Directed collective motion of bacteria under channel confinement. *New J. Phys.* 18:075002
76. Licata NA, Mohari B, Fuqua C, Setayeshgar S. 2016. Diffusion of bacterial cells in porous media. *Biophys. J.* 110:247–57
77. Liu J, Ford RM, Smith JA. 2011. Idling time of motile bacteria contributes to retardation and dispersion in sand porous medium. *Environ. Sci. Technol.* 45:3945–51
78. Maennik J, Driessens R, Galajda P, Keymer JE, Dekker C. 2009. Bacterial growth and motility in sub-micron constrictions. *PNAS* 106:14861–66
79. Cisneros L, Dombrowski C, Goldstein RE, Kessler JO. 2006. Reversal of bacterial locomotion at an obstacle. *Phys. Rev. E* 73:030901
80. Magariyama Y, Ichiba M, Nakata K, Baba K, Ohtani T, et al. 2008. Difference in bacterial motion between forward and backward swimming caused by the wall effect. *Biophys. J.* 88:3648–58
81. Sosa-Hernández JE, Santillán M, Santana-Solano J. 2017. Motility of *Escherichia coli* in a quasi-two-dimensional porous medium. *Phys. Rev. E* 95:032404
82. Raatz M, Hintsche M, Bahrs M, Theves M, Beta C. 2015. Swimming patterns of a polarly flagellated bacterium in environments of increasing complexity. *Eur. Phys. J. Spec. Top.* 224:1185–98
83. Jabbarzadeh M, Hyon Y, Fu HC. 2014. Swimming fluctuations of micro-organisms due to heterogeneous microstructure. *Phys. Rev. E* 90:043021
84. Schneider WR, Doetsch RN. 1974. Effect of viscosity on bacterial motility. *J. Bacteriol.* 117:696–701

85. Martinez VA, Schwarz-Linek J, Reufer M, Wilson LG, Morozov AN, Poon WCK. 2014. Flagellated bacterial motility in polymer solutions. *PNAS* 111:17771–76
86. Patteson AE, Gopinath A, Goulian M, Arratia PE. 2015. Running and tumbling with *E. coli* in polymeric solutions. *Sci. Rep.* 5:15761
87. Li GJ, Karimi A, Ardekani AM. 2014. Effect of solid boundaries on swimming dynamics of microorganisms in a viscoelastic fluid. *Rheol. Acta* 53:911–26
88. Li G, Ardekani AM. 2016. Collective motion of microorganisms in a viscoelastic fluid. *Phys. Rev. Lett.* 117:118001
89. Celli JP, Turner BS, Afdhal NH, Keates S, Ghiran I, et al. 2009. *Helicobacter pylori* moves through mucus by reducing mucin viscoelasticity. *PNAS* 106:14321–26
90. Kimsey RB, Spielman A. 1990. Motility of Lyme disease spirochetes in fluids as viscous as the extracellular matrix. *J. Infect. Dis.* 162:1205–8
91. Mathijssen AJTM, Shendruk TN, Yeomans JM, Doostmohammadi A. 2016. Upstream swimming in microbiological flows. *Phys. Rev. Lett.* 116:028104
92. Bakker DP, Busscher HJ, van der Mei HC. 2002. Bacterial deposition in a parallel plate and a stagnation point flow chamber: Microbial adhesion mechanisms depend on the mass transport conditions. *Microbiology* 148:597–603
93. Swartjes JJTM, Veerdegowda DH, van der Mei HC, Busscher HJ, Sharma PK. 2014. Normally oriented adhesion versus friction forces in bacterial adhesion to polymer-brush functionalized surfaces under fluid flow. *Adv. Funct. Mater.* 24:4435–41
94. O'Toole GA, Wong GCL. 2016. Sensational biofilms: surface sensing in bacteria. *Curr. Opin. Microbiol.* 30:139–46
95. Janissen R, Murillo DM, Niza B, Sahoo PK, Nobrega MM, et al. 2015. Spatiotemporal distribution of different extracellular polymeric substances and filamentation mediate *Xylella fastidiosa* adhesion and biofilm formation. *Sci. Rep.* 5:9856
96. Perni S, Preedy EC, Prokopovich P. 2014. Success and failure of colloidal approaches in adhesion of microorganisms to surfaces. *Adv. Colloid Interface Sci.* 206:265–74
97. Forero M, Thomas WE, Bland C, Nilsson LM, Sokurenko EV, Vogel V. 2004. A catch-bond based nanoadhesive sensitive to shear stress. *Nano Lett.* 4:1593–97
98. Thomas WE, Trintchina E, Forero M, Vogel V, Sokurenko EV. 2002. Bacterial adhesion to target cells enhanced by shear force. *Cell* 109:913–23
99. Lecuyer S, Rusconi R, Shen Y, Forsyth AM, Vlamakis H, et al. 2011. Shear stress increases the residence time of adhesion of *Pseudomonas aeruginosa*. *Biophys. J.* 100:341–50
100. Sharma S, Jaimes-Lizcano YA, McLay RB, Cirino PC, Conrad JC. 2016. Subnanometric roughness affects the deposition and mobile adhesion of *Escherichia coli* on silanized glass surfaces. *Langmuir* 32:5422–33
101. Thomas WE, Nilsson LM, Forero M, Sokurenko EV, Vogel V. 2004. Shear-dependent “stick-and-roll” adhesion of type 1 fimbriated *Escherichia coli*. *Mol. Microbiol.* 53:1545–57
102. Anderson BN, Ding AM, Nilsson LM, Kusuma K, Tchesnokova V, et al. 2007. Weak rolling adhesion enhances bacterial surface colonization. *J. Bacteriol.* 189:1794–802
103. Boks NP, Kaper HJ, Norde W, van der Mei HC, Busscher HJ. 2009. Mobile and immobile adhesion of staphylococcal strains to hydrophilic and hydrophobic surfaces. *J. Colloid Interface Sci.* 331:60–64
104. McClaine JW, Ford RM. 2002. Characterizing the adhesion of motile and nonmotile *Escherichia coli* to a glass surface using a parallel-plate flow chamber. *Biotechnol. Bioeng.* 78:179–89
105. de Kerchove AJ, Elimelech M. 2008. Bacterial swimming motility enhances cell deposition and surface coverage. *Environ. Sci. Technol.* 42:4371–77
106. Lu N, Massoudieh A, Liang X, Hu D, Kamai T, et al. 2015. Swimming motility reduces *Azotobacter vinelandii* deposition to silica surfaces. *J. Environ. Qual.* 44:1366–75
107. Friedlander RS, Vlamakis H, Kim P, Khan M, Kolter R, Aizenberg J. 2013. Bacterial flagella explore microscale hummocks and hollows to increase adhesion. *PNAS* 110:5624–29
108. Neuman KC, Chadd EH, Liou G, Bergman K, Block SM. 1999. Characterization of photodamage to *Escherichia coli* in optical traps. *Biophys. J.* 77:2856–63

109. Conrad JC, Gibiansky ML, Jin F, Gordon VD, Motto DA, et al. 2011. Flagella and pili-mediated near-surface single-cell motility mechanisms in *P. aeruginosa*. *Biophys. J.* 100:1608–16
110. Bennett RR, Lee CK, De Anda J, Nealson KH, Yildiz FH, et al. 2016. Species-dependent hydrodynamics of flagellum-tethered bacteria in early biofilm development. *J. R. Soc. Interface* 13:20150966
111. Sharma S, Conrad JC. 2014. Attachment from flow of *Escherichia coli* bacteria onto silanized glass substrates. *Langmuir* 30:11147–55
112. de Anda J, Lee EY, Lee CK, Bennett RR, Ji X, et al. 2017. High-speed “4D” computational microscopy of bacterial suspensions. *ACS Nano* 11:9340–51
113. Skerker JM, Berg HC. 2001. Direction observation of extension and retraction of type IV pili. *PNAS* 98:6901–4
114. Utada AS, Bennett RR, Fong JCN, Gibiansky ML, Yildiz FH, et al. 2014. *Vibrio cholerae* use pili and flagella synergistically to effect motility switching and conditional surface attachment. *Nat. Commun.* 5:4913
115. Golovkine G, Lemelle L, Burny C, Vaillant C, Palierne JF, et al. 2016. Host cell surfaces induce a type IV pili-dependent alteration of bacterial swimming. *Sci. Rep.* 6:38950
116. Gibiansky ML, Conrad JC, Jin F, Gordon VD, Motto DA, et al. 2010. Bacteria use type IV pili to walk upright and detach from surfaces. *Science* 330:197
117. Shen Y, Siryaporn A, Lecuyer S, Gitai Z, Stone HA. 2012. Flow directs surface-attached bacteria to twitch upstream. *Biophys. J.* 103:146–51
118. Meng Y, Li Y, Galvani CD, Hao G, Turner JN, et al. 2005. Upstream migration of *Xylella fastidiosa* via pilus-driven twitching motility. *J. Bacteriol.* 187:5560–67
119. Bahar O, De La Fuente L, Burdman S. 2010. Assessing adhesion, biofilm formation and motility of *Acidovorax citrulli* using microfluidic flow chambers. *FEMS Microbiol. Lett.* 312:33–39
120. Siryaporn A, Kim MK, Shen Y, Stone HA, Gitai Z. 2015. Colonization, competition, and dispersal of pathogens in fluid flow networks. *Curr. Biol.* 25:1201–7
121. Jin F, Conrad JC, Gibiansky ML, Wong GCL. 2011. Bacteria use type-IV pili to slingshot on surfaces. *PNAS* 108:12617–22
122. Meel C, Kouzel N, Oldewurtel ER, Maier B. 2012. Three-dimensional obstacles for bacterial surface motility. *Small* 8:530–34
123. Holz C, Opitz D, Mehlich J, Ravoo BJ, Maier B. 2009. Bacterial motility and clustering guided by microcontact printing. *Nano Lett.* 9:4553–57
124. Zhang R, Ni L, Jin Z, Li J, Jin F. 2014. Bacteria slingshot more on soft surfaces. *Nat. Commun.* 5:5541
125. Persat A, Inclan YF, Engel JN, Stone HA, Gitai Z. 2015. Type IV pili mechanochemically regulate virulence factors in *Pseudomonas aeruginosa*. *PNAS* 112:7563–68
126. Rodesney CA, Roman B, Dhamani N, Cooley BJ, Touhami A, Gordon VD. 2017. Mechanosensing of shear by *Pseudomonas aeruginosa* leads to increased levels of the cyclic-di-GMP signal initiating biofilm development. *PNAS* 114:5906–11
127. Epstein AK, Wong TS, Belisle RA, Boggs EM, Aizenberg J. 2012. Liquid-infused structured surfaces with exceptional anti-biofouling performance. *PNAS* 109:13182–87
128. Wloka M, Rehage H, Flemming HC, Wingender J. 2004. Rheological properties of viscoelastic biofilm extracellular polymeric substances and comparison to the behavior of calcium alginate gels. *Colloid Polymer Sci.* 282:1067–76
129. Ganesan M, Knier S, Younger JG, Solomon MJ. 2016. Associative and entanglement contributions to the solution rheology of a bacterial polysaccharide. *Macromolecules* 49:8313–21
130. Zhao K, Tseng BS, Beckerman B, Jin F, Gibiansky ML, et al. 2013. Psl trails guide exploration and microcolony formation in *Pseudomonas aeruginosa* biofilms. *Nature* 497:388–92
131. Wang H, Sodagari M, Ju LK, Newby BMZ. 2013. Effects of shear on initial bacterial attachment in slow flowing systems. *Colloid Surf. B* 109:32–39
132. Haznedaroglu BZ, Bolster CH, Walker SL. 2008. The role of starvation on *Escherichia coli* adhesion and transport in saturated porous media. *Water Res.* 42:1547–54
133. Song L, Sjollema J, Sharma PK, Kaper HJ, van der Mei HC, Busscher HJ. 2014. Nanoscopic vibrations of bacteria with different cell-wall properties adhering to surfaces under flow and static conditions. *ACS Nano* 8:8457–67

134. Weiss TH, Mills AL, Hornberger GM, Herman JS. 1995. Effect of bacterial cell shape on transport of bacteria in porous media. *Environ. Sci. Technol.* 29:1737–40
135. Persat A, Stone HA, Gitai Z. 2014. The curved shape of *Caulobacter crescentus* enhances surface colonization in flow. *Nat. Commun.* 5:3824
136. Picioreanu C, Van Loosdrecht MCM, Heijnen JJ. 2000. Effect of diffusive and convective substrate transport on biofilm structure formation: a two-dimensional modeling study. *Biotechnol. Bioeng.* 69:504–15
137. Weaver WM, Milisavljevic V, Miller JF, Di Carlo D. 2012. Fluid flow induces biofilm formation in *Staphylococcus epidermidis* polysaccharide intracellular adhesin-positive clinical isolates. *Appl. Environ. Microbiol.* 78:5890–96
138. Maier B, Potter L, So M, Long CD, Seifert HS, Sheetz MP. 2002. Single pilus motor forces exceed 100 pN. *PNAS* 99:16012–17
139. Billings N, Birjiniuk A, Samad TS, Doyle PS, Ribbeck K. 2015. Material properties of biofilms: a review of methods for understanding permeability and mechanics. *Rep. Prog. Phys.* 78:036601–18
140. Shaw T, Winston M, Rupp CJ, Klapper I, Stoodley P. 2004. Commonality of elastic relaxation times in biofilms. *Phys. Rev. Lett.* 93:098102
141. Pavlovsky L, Younger JG, Solomon MJ. 2013. In situ rheology of *Staphylococcus epidermidis* bacterial biofilms. *Soft Matter* 9:122–31
142. Chen M, Zhang Z, Bott T. 1998. Direct measurement of the adhesive strength of biofilms in pipes by micromanipulation. *Biotechnol. Tech.* 12:875–80
143. Kostenko V, Salek MM, Sattari P, Martinuzzi RJ. 2010. *Staphylococcus aureus* biofilm formation and tolerance to antibiotics in response to oscillatory shear stresses of physiological levels. *FEMS Immunol. Med. Microbiol.* 59:421–31
144. Vieira MJ, Melo LF, Pinheiro MM. 1993. Biofilm formation: hydrodynamic effects on internal diffusion and structure. *Biofouling* 7:67–80
145. Stoodley P, Jacobsen A, Dunsmore BC, Purevdorj B, Wilson S, et al. 2001. The influence of fluid shear and AlCl₃ on the material properties of *Pseudomonas aeruginosa* PAO1 and *Desulfovibrio* sp. EX265 biofilms. *Water Sci. Technol.* 43:113–20
146. Dunsmore BC, Jacobsen A, Hall-Stoodley L, Bass CJ, Lappin-Scott HM, Stoodley P. 2002. The influence of fluid shear on the structure and material properties of sulphate-reducing bacterial biofilms. *J. Ind. Microbiol. Biotechnol.* 29:347–53
147. Paramonova E, Kalmykowa OJ, van der Mei HC, Busscher HJ, Sharma PK. 2009. Impact of hydrodynamics on oral biofilm strength. *J. Dent. Res.* 88:922–26
148. Purevdorj B, Costerton JW, Stoodley P. 2002. Influence of hydrodynamics and cell signaling on the structure and behavior of *Pseudomonas aeruginosa* biofilms. *Appl. Environ. Microbiol.* 68:4457–64
149. Choi YC, Morgenroth E. 2003. Monitoring biofilm detachment under dynamic changes in shear stress using laser-based particle size analysis and mass fractionation. *Water Sci. Technol.* 47:69–76
150. Stoodley P, Cargo R, Rupp CJ, Wilson S, Klapper I. 2002. Biofilm material properties as related to shear-induced deformation and detachment phenomena. *J. Ind. Microbiol. Biotechnol.* 29:361–67
151. Rupp CJ, Fux CA, Stoodley P. 2005. Viscoelasticity of *Staphylococcus aureus* biofilms in response to fluid shear allows resistance to detachment and facilitates rolling migration. *Appl. Environ. Microbiol.* 71:2175–78
152. Rusconi R, Lecuyer S, Autrusson N, Guglielmini L, Stone HA. 2011. Secondary flow as a mechanism for the formation of biofilm streamers. *Biophys. J.* 100:1392–99
153. Hassanpourfard M, Ghosh R, Thundat T, Kumar A. 2016. Dynamics of bacterial streamers induced clogging in microfluidic devices. *Lab Chip* 16:4091–96
154. Stoodley P, Lewandowski Z, Boyle JD, Lappin-Scott HM. 1999. Structural deformation of bacterial biofilms caused by short-term fluctuations in fluid shear: an in situ investigation of biofilm rheology. *Biotechnol. Bioeng.* 65:83–92
155. Kim MK, Drescher K, Pak OS, Bassler BL, Stone HA. 2014. Filaments in curved streamlines: rapid formation of *Staphylococcus aureus* biofilm streamers. *New J. Phys.* 16:065204
156. Yazdi S, Ardekani AM. 2012. Bacterial aggregation and biofilm formation in a vortical flow. *Biomicrofluidics* 6:044114

157. Rusconi R, Lecuyer S, Guglielmini L, Stone HA. 2010. Laminar flow around corners triggers the formation of biofilm streamers. *J. R. Soc. Interface* 7:1293–99
158. Hassanpourfard M, Nikakhtari Z, Ghosh R, Das S, Thundat T, et al. 2015. Bacterial floc mediated rapid streamer formation in creeping flows. *Sci. Rep.* 5:13070
159. Drescher K, Shen Y, Bassler BL, Stone HA. 2013. Biofilm streamers cause catastrophic disruption of flow with consequences for environmental and medical systems. *PNAS* 110:4345–50
160. Kumar A, Karig D, Acharya R, Neethirajan S, Mukherjee PP, et al. 2013. Microscale confinement features can affect biofilm formation. *Microfluid. Nanofluid.* 14:895–902
161. Bottero S, Storck T, Heimovaara TJ, van Loosdrecht MC, Enzien MV, Picoreanu C. 2013. Biofilm development and the dynamics of preferential flow paths in porous media. *Biofouling* 29:1069–86
162. Peszynska M, Trykozko A, Iltis G, Schlueter S, Wildenschild D. 2016. Biofilm growth in porous media: experiments, computational modeling at the porescale, and upscaling. *Adv. Water Resour.* 95:288–301
163. Coyte KZ, Tabuteau H, Gaffney EA, Foster KR, Durham WM. 2017. Microbial competition in porous environments can select against rapid biofilm growth. *PNAS* 114:E161–70
164. Nadell CD, Ricaurte D, Yan J, Drescher K, Bassler BL. 2017. Flow environment and matrix structure interact to determine spatial competition in *Pseudomonas aeruginosa* biofilms. *eLife* 6:e21855
165. Stewart PS. 2003. Diffusion in biofilms. *J. Bacteriol.* 185:1485–91
166. Stoodley P, Yang S, Lappin-Scott H, Lewandowski Z. 1997. Relationship between mass transfer coefficient and liquid flow velocity in heterogenous biofilms using microelectrodes and confocal microscopy. *Biotechnol. Bioeng.* 56:681–88
167. Beyenal H, Lewandowski Z. 2002. Internal and external mass transfer in biofilms grown at various flow velocities. *Biotechnol. Prog.* 18:55–61
168. Stanley NR, Lazazzera BA. 2004. Environmental signals and regulatory pathways that influence biofilm formation. *Mol. Microbiol.* 52:917–24
169. Waters CM, Bassler BL. 2005. Quorum sensing: cell-to-cell communication in bacteria. *Annu. Rev. Cell Dev. Biol.* 21:319–46
170. Connell JL, Wessel AK, Parsek MR, Ellington AD, Whiteley M, Shear JB. 2010. Probing prokaryotic social behaviors with bacterial “lobster traps.” *mBio* 1:e00202
171. Dulla G, Lindow SE. 2008. Quorum size of *Pseudomonas syringae* is small and dictated by water availability on the leaf surface. *PNAS* 105:3082–87
172. Ribbe J, Maier B. 2016. Density-dependent differentiation of bacteria in spatially structured open systems. *Biophys. J.* 110:1648–60
173. Boedicker JQ, Vincent ME, Ismagilov RF. 2009. Microfluidic confinement of single cells of bacteria in small volumes initiates high-density behavior of quorum sensing and growth and reveals its variability. *Angew. Chem. Int. Ed.* 48:5908–11
174. Carnes EC, Lopez DM, Donegan NP, Cheung A, Gresham H, et al. 2010. Confinement-induced quorum sensing of individual *Staphylococcus aureus* bacteria. *Nat. Chem. Biol.* 6:41–45
175. Kirisits MJ, Margolis JJ, Purevdorj-Gage BL, Vaughan B, Chopp DL, et al. 2007. Influence of the hydrodynamic environment on quorum sensing in *Pseudomonas aeruginosa* biofilms. *J. Bacteriol.* 189:8357–60
176. Kim MK, Ingremeau F, Zhao A, Bassler BL, Stone HA. 2016. Local and global consequences of flow on bacterial quorum sensing. *Nat. Microbiol.* 1:15005
177. Emge P, Moeller J, Jang H, Rusconi R, Yawata Y, et al. 2016. Resilience of bacterial quorum sensing against fluid flow. *Sci. Rep.* 6:33115
178. Zhao J, Wang Q. 2017. Three-dimensional numerical simulations of biofilm dynamics with quorum sensing in a flow cell. *Bull. Math. Biol.* 79:884–919

Contents

Autobiography of Ronald W. Rousseau <i>Ronald W. Rousseau</i>	1
Single- to Few-Layered, Graphene-Based Separation Membranes <i>Fanglei Zhou, Mabdi Fathizadeh, and Miao Yu</i>	17
From Multiscale to Mesoscience: Addressing Mesoscales in Mesoregimes of Different Levels <i>Jinghai Li and Wenhai Huang</i>	41
Toward Constitutive Models for Momentum, Species, and Energy Transport in Gas-Particle Flows <i>Sankaran Sundaresan, Ali Ozel, and Jari Kolehmainen</i>	61
Stable Radical Materials for Energy Applications <i>Daniel A. Wilcox, Varad Agarkar, Sanjoy Mukherjee, and Bryan W. Boudouris</i>	83
Biodegradable Polymeric Nanoparticles for Therapeutic Cancer Treatments <i>Johan Karlsson, Hannah J. Vaughan, and Jordan J. Green</i>	105
Critical Comparison of Structured Contactors for Adsorption-Based Gas Separations <i>Stephen J.A. DeWitt, Anshuman Sinha, Jayashree Kalyanaraman, Fengyi Zhang, Matthew J. Realff, and Ryan P. Lively</i>	129
The Energy Future <i>John Newman, Christopher A. Bonino, and James A. Trainham</i>	153
Confined Flow: Consequences and Implications for Bacteria and Biofilms <i>Jacinta C. Conrad and Ryan Poling-Skutvik</i>	175
Molecular Modelling for Reactor Design <i>Frerich J. Keil</i>	201
Biomolecular Ultrasound and Sonogenetics <i>David Maresca, Anupama Lakshmanan, Mohamad Abedi, Avinoam Bar-Zion, Arash Farhadi, George J. Lu, Jerzy O. Szablowski, Di Wu, Sangjin Yoo, and Mikhail G. Shapiro</i>	229

Continuous Manufacturing in Pharmaceutical Process Development and Manufacturing <i>Christopher L. Burcham, Alastair J. Florence, and Martin D. Johnson</i>	253
Crystal Engineering for Catalysis <i>Jeffrey D. Rimer, Aseem Chawla, and Thuy T. Le</i>	283
Engineered Ribosomes for Basic Science and Synthetic Biology <i>Anne E. d'Aquino, Do Soon Kim, and Michael C. Jewett</i>	311
Shale Gas Implications for C ₂ -C ₃ Olefin Production: Incumbent and Future Technology <i>Eric E. Stangland</i>	341
Nanoscale Optical Microscopy and Spectroscopy Using Near-Field Probes <i>Richard J. Hermann and Michael J. Gordon</i>	365
Advances in Multicompartment Mesoporous Silica Micro/Nanoparticles for Theranostic Applications <i>Jian Liu, Tingting Liu, Jian Pan, Shaomin Liu, and G.Q. (Max) Lu</i>	389
Microkinetic Analysis and Scaling Relations for Catalyst Design <i>Ali Hussain Motagamwala, Madelyn R. Ball, and James A. Dumesic</i>	413

Indexes

Cumulative Index of Contributing Authors, Volumes 5–9	451
Cumulative Index of Article Titles, Volumes 5–9	454

Errata

An online log of corrections to *Annual Review of Chemical and Biomolecular Engineering* articles may be found at <http://www.annualreviews.org/errata/chembioeng>